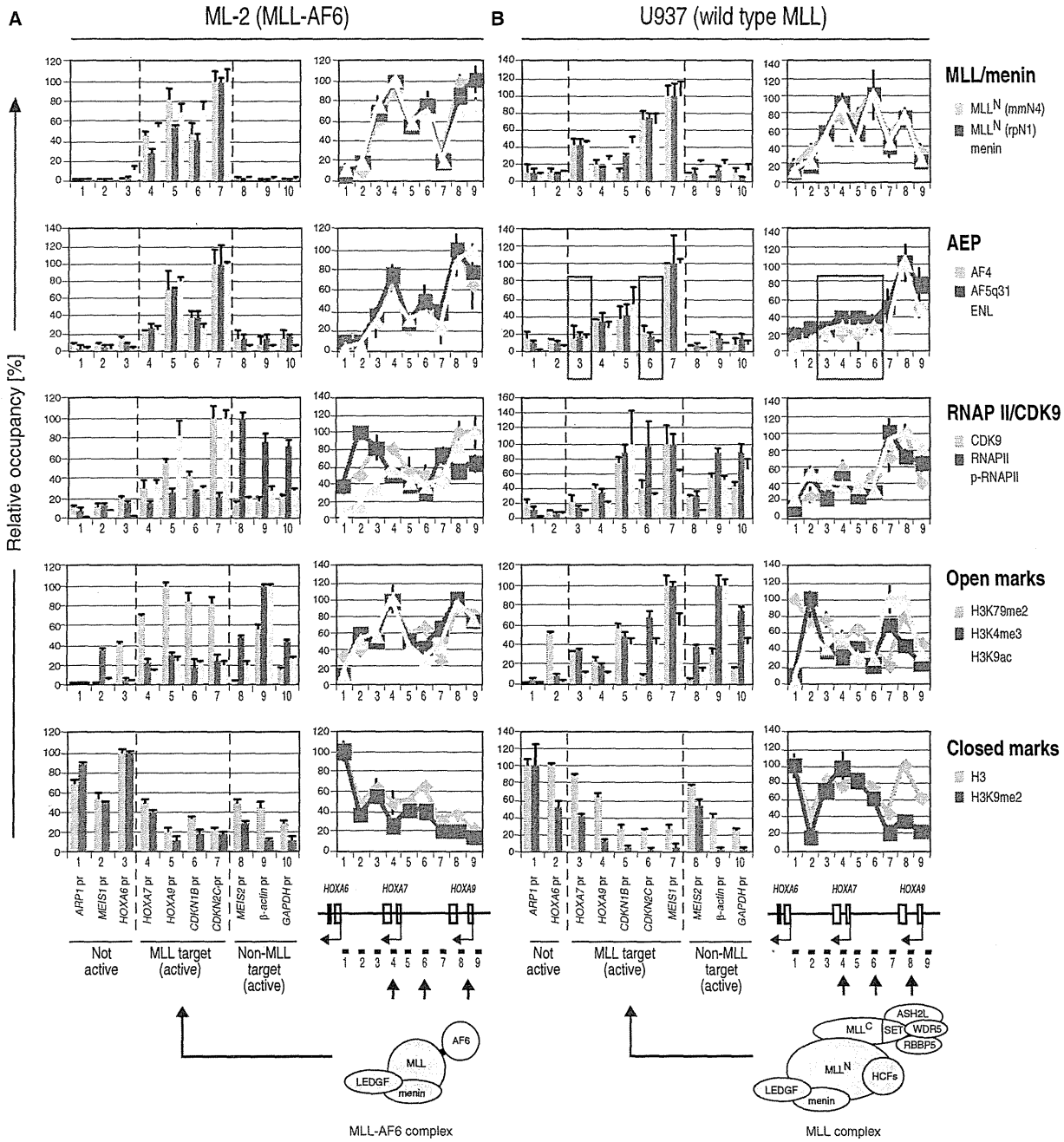

Figure 6. Indirect Recruitment of AEP to MLL-AF6- or WT MLL-Occupied Loci

(A and B) Genomic localizations of indicated proteins in ML-2 (A) and U937 (B) cells were determined by ChIP assay as in Figure 2B. The purple rectangle highlights regions where AEP is absent while the MLL complexes are present. ChIP data using anti-MLL^N (rpN1) and anti-menin antibodies are partially adapted from a previous report (Yokoyama and Cleary, 2008). See also Figure S5.

with AEP at the chromatin of MLL target genes (*HOXA7*, *HOXA9*, *CDKN1B*, and *CDKN2C*) (Figure 6A and Figure S5A) despite its inability to directly associate with AEP (Figures 1E and 5C). The occupancies of CDK9 and phosphorylated RNAPII coincided with the presence of AEP on MLL-AF6 target genes (Figure 6A). Characteristically, high levels of dimethyl H3K79 were associated with the presence of AEP, corroborating the functional link between AEP and DOT1L. These results suggest

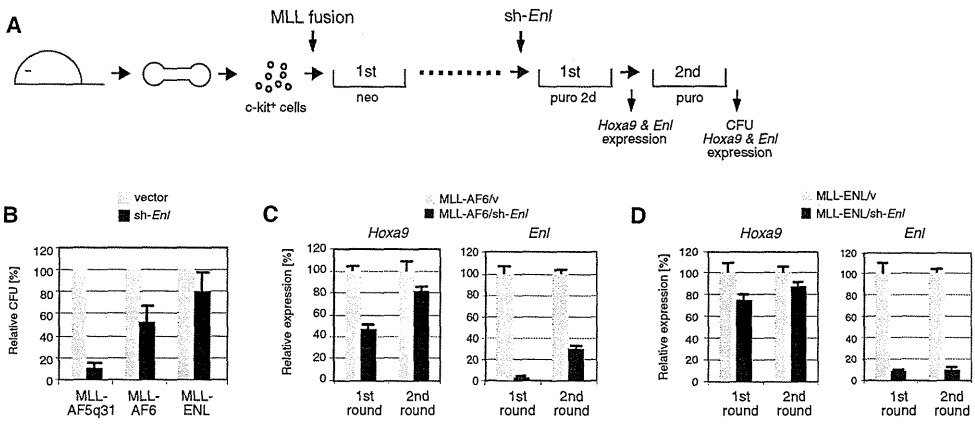

Figure 7. ENL Is Required for MLL-AF6-Dependent Transactivation and Transformation

(A) The experimental scheme to evaluate the effect of *Enl* knockdown on MLL transformation is shown.

(B) Clonogenic potentials are shown for myeloid cells transformed by MLL oncogenes (indicated below) at the second plating after sh-RNA transduction (vector or sh-*Enl*). CFU numbers are displayed relative to the vector control arbitrarily set as 100. Error bars represent standard deviations of three independent analyses.

(C) MLL-AF6-transformed cells from first- and second-round colonies following sh-RNA transduction (vector or sh-*Enl*) were analyzed by RT-PCR for expression of endogenous *Enl* or *Hoxa9*. Expression levels were normalized to *GAPDH* levels and are displayed relative to the transcript levels in vector control cells arbitrarily set as 100. Error bars represent standard deviations of triplicate PCRs.

(D) The same analysis as (C) was performed on MLL-ENL-transformed cells. Note that data in (B) and (D) are partially redundant with Figures 3I and 3J.

that the AEP complex can be recruited to MLL target loci via an indirect mechanism potentially serving a role in MLL-AF6-dependent leukemogenesis.

MLL-AF6-transformed cells were also dependent on Enl, because its knockdown reduced their clonogenicity and *Hoxa9* expression by 50% (Figures 7A and 7C). This was less severe, compared with MLL-AF5q31-transformed cells (Figure 7B), in part because of insufficient knockdown by the sh-RNA, since secondary colonies expressed *Hoxa9* at its normal levels accompanied with impaired knockdown of *Enl* (Figure 7C), indicating a selective proliferative advantage of cells in which *Enl* was incompletely knocked down (MLL-ENL served as a negative control in Figure 7D). Thus, transformation by MLL-AF6 is dependent on ENL, despite an inability to directly associate with AEP.

AEP Facilitates the Physiologic MLL-Dependent Transcriptional Pathway

The foregoing results prompted studies of a potential relationship of AEP in physiologic transcriptional regulation by WT MLL. ChIP analyses of U937 cells, which lack an MLL chromosomal translocation (Dreyling et al., 1996; Guenther et al., 2005), showed that AEP colocalized with WT MLL at the *HOXA9*, *MEIS1*, and *CDKN1B* promoters (Figure 6B and Figure S5B). However, in contrast to MLL leukemia cell lines, colocalization was not observed at all of the MLL-occupied loci in U937 cells. For instance, the MLL complex occupied both the *HOXA7* and *HOXA9* loci, whereas AEP associated only with the latter (Figure 6B, purple rectangle). A similar disparity was observed at the *CDKN2C* promoter. These results suggest that AEP is recruited to WT MLL-occupied loci in a context-dependent manner, as opposed to its constitutive recruitment in MLL leukemia cells. The presence of AEP correlated more closely with active transcriptional marks such as phospho-RNAPII and acetyl-histone H3K9 (e.g., the *HOXA7-9* locus), suggesting that AEP recruitment to MLL-targeted chromatin facilitates transcription.

The role of ENL in physiologic MLL-dependent transcriptional maintenance was assessed by knocking down *Enl* in mouse embryonic fibroblasts (MEFs), in which *Hoxc8* is a target gene of the Mll/menin complex (Figure 8A) (Hughes et al., 2004; Milne et al., 2002). *Enl* knockdown caused reduction of *Hoxc8* expression, which could be prevented by antecedent expression of exogenous human ENL (Figure 8B). Thus, Enl is required for physiologic transcriptional regulation by the Mll/menin complex. Moreover, Dot1l-mediated histone methylation was decreased at the Hoxc8 promoter in *Men1* null MEFs (Figure 8C), indicating that the MLL/menin complex functions upstream of ENL/DOT1L functions.

Furthermore, *ENL* knockdown in U937 cells caused downregulation of *HOXA9*, *CDKN1B*, and *MEIS1*, whose genomic loci were occupied by both MLL and AEP complexes, but did not affect expression of genes occupied by the MLL complex without AEP (*HOXA7* and *CDKN2C*) (*AF5q31*, *MLL*, or *β-ACTIN* served as negative controls) (Figures 6B and 8D). Thus, ENL is specifically required for the optimal transcription of genes occupied by both MLL and AEP complexes.

DISCUSSION

Our biochemical purification of AF4 family proteins demonstrates that they normally associate with ENL and the P-TEFb elongation factor in an endogenous complex (AEP) in hematopoietic cells. MLL oncoproteins fused with AEP components (AF4 or ENL family proteins) nucleate formation of MLL/AEP hybrid complexes that constitutively occupy MLL-target chromatin. This aberrant recruitment of AEP components causes sustained activation of MLL target gene transcription and transformation of hematopoietic progenitors. Although the AEP and

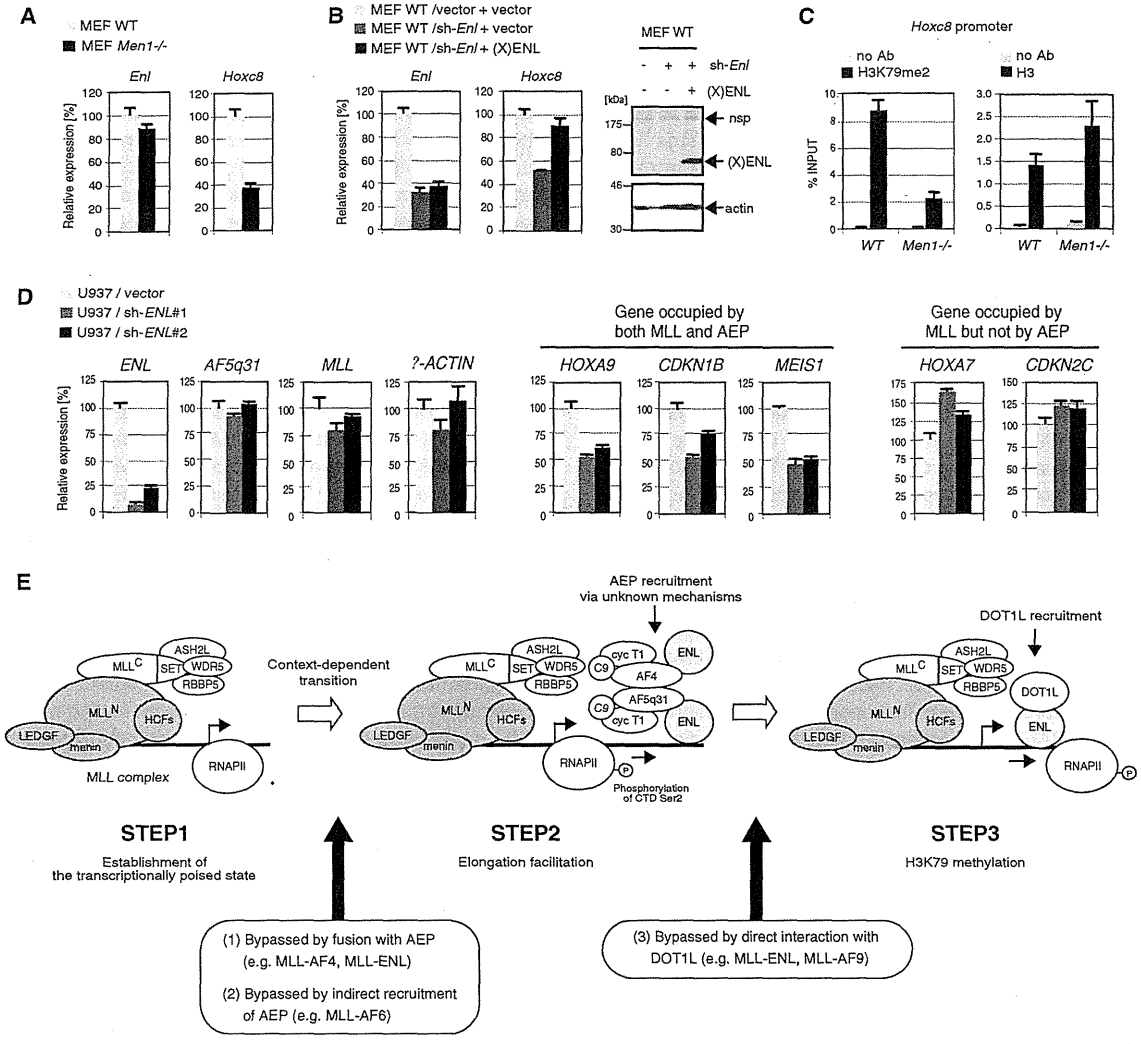

Figure 8. ENL Functions Downstream of Physiologic MLL-Dependent Transcriptional Pathways

(A) Expression levels of *Enl* and *Hoxc8* in WT or *Men1*$^{-/-}$ MEFs were determined by RT-PCR (normalized to *β-actin* levels and are displayed relative to the vector control arbitrarily set as 100). Error bars represent standard deviations of triplicate PCRs.

(B) Expression of *Enl* and *Hoxc8* with or without *Enl* knockdown/rescue was determined by RT-PCR. Expression levels were normalized to *β-actin* levels and are expressed relative to the vector/vector control arbitrarily set as 100. Error bars represent standard deviations of triplicate PCRs. Protein levels of the exogenously expressed (X)ENL (right panels) were assessed by western blotting with an anti-Xpress antibody (actin immunoblot served as a loading control). nsp, nonspecific band.

(C) ChIP assay was performed on WT or *Men1*$^{-/-}$ MEFs using anti-dimethyl H3K79 and histone H3 antibodies for the *Hoxc8* promoter-adjacent region and results displayed as relative ratio (%) to the input DNA. Error bars represent standard deviations of triplicate PCRs.

(D) The effects of *ENL*-knockdown are shown for two different sh-RNAs in U937 cells. Expression of various genes was analyzed by RT-PCR 4 days after transduction/puromycin selection. Expression values were normalized to *GAPDH* levels and displayed relative to the vector control arbitrarily set as 100. Error bars represent standard deviations of triplicate PCRs.

(E) A three-step model of MLL-dependent transcription.

MLL complexes are normally separate biochemical entities, our studies support a dependent role for the AEP complex in physiologic MLL target gene expression pathways, whose conditional recruitment mechanisms are often bypassed by leukemic MLL fusion proteins.

The AEP complex purified from leukemia cell lines under our experimental conditions contained ENL as an integral component but lacked a number of previously reported ENL-associated proteins, most notably the DOT1L histone methyltransferase (Mueller et al., 2007). Our domain-mapping analyses provide a molecular basis for its absence in that DOT1L and AF4 family proteins use the same binding surface within the AHD of ENL. Because of this physical constraint, DOT1L and AF4 family proteins are incapable of simultaneously associating with the

AHD to form an AF4/ENL/DOT1L trimeric complex. Therefore, retention of DOT1L in the AF4 complex previously identified in thymus homogenates (Bitoun et al., 2007) is likely mediated by other proteins (e.g., AF10 and RNAPII) but not by ENL/AF9. Our data suggest that an endogenous ENL/DOT1L complex and AEP normally exist as separate entities consistent with previous suggestions that ENL may participate in a mixture of different subcomplexes (Mueller et al., 2007).

A role for ENL in multiple subcomplexes raises the issue of which of its molecular interactions is essential for MLL leukemogenesis. This issue was addressed by assessing the oncogenic potential of MLL fused with the DOT1L catalytic domain, which effectively bypasses ENL. Contrary to a previous report (Okada et al., 2005), MLL-DOT1L was not sufficient for transactivation of MLL target genes and transformation of myeloid progenitors under our experimental conditions that read out the oncogenic properties of MLL-AF5q31 and MLL-ENL. This finding indicates that aberrant recruitment of AEP, not DOT1L, plays a primary rate-limiting role in transactivation and transformation by MLL fusion proteins, a conclusion further supported by structure/function analysis of MLL-AF5q31 showing that its CHD, which mediates hetero-interactions with AF4 family members, was necessary and sufficient for transformation.

Nevertheless, ChIP analyses by us and others show that H3K79 methylation marks are present at most MLL-AF4-target loci (Figure 2B) (Krivtsov et al., 2008; Guenther et al., 2008), indicating that there is a strong functional interconnection between AEP and DOT1L. DOT1L-dependent H3K79 methylation is associated with transcribed regions and stimulated by histone H2B K120 mono-ubiquitination (a histone mark accompanied with transcription), but is not required for transcription itself (Steger et al., 2008; McGinty et al., 2008). This finding suggests that DOT1L-dependent H3K79 methylation occurs after the traverse of RNAPII and may play roles in the maintenance of transcriptional memory rather than initiating transcription per se. In this context, our studies support dual roles for ENL, which is capable of interacting with AEP or DOT1L through its AHD to sequentially recruit them to the same target chromatin, possibly via its N-terminal YEATS domain that retains a chromatin binding property (Zeisig et al., 2005).

Our data demonstrate that AEP colocalizes with WT MLL on target promoters indicative of a role in physiologic as well as oncogenic MLL-dependent transcriptional pathways. Supporting this notion, knockdown of *ENL* impaired expression of MLL target genes in MEFs and U937 cells (Figures 8B and 8D), and *Af9*-deficient mice display homeotic transformations similar to those of *Mll*-deficient mice (Collins et al., 2002). The recruitment of AEP to MLL-target loci appears to be nonconstitutive because some MLL-occupied loci do not contain AEP (Figure 6B). Because the presence of the MLL complex does not invariably correlate with occupancy by AEP, other factors or signals yet to be identified are likely required for AEP recruitment. On the basis of these observations and speculations, we propose a three-step model in which WT MLL first establishes/maintains the transcriptionally poised state (Step 1), AEP is then recruited to facilitate onset of transcriptional initiation and/or elongation (Step 2), which is followed by DOT1L-dependent H3K79 methylation post-transcription (Step 3) (Figure 8E). In this model, ENL serves a key role in sequential recruitment of AEP and DOT1L, respectively.

To date, up to 50 different proteins have been reported to fuse with *MLL* in human leukemias. This promiscuity poses a question as to whether any common trait is shared among the fusion partners. We demonstrate here that AEP recruitment is a downstream event in physiologic MLL-dependent transcriptional pathways and is regulated in a context-dependent manner. MLL-AF4 and MLL-ENL family fusions transform myeloid progenitors by constitutively recruiting AEP to MLL-target loci through direct association. Thus, one of the major mechanisms of MLL-dependent transformation is constitutive activation of MLL-dependent transcription by direct recruitment of AEP, which circumvents the regulatory mechanisms that normally control AEP recruitment (Figure 8E).

AEP does not physically interact with MLL-AF6, but nevertheless consistently colocalizes with MLL-AF6 at target chromatin to activate transcription (Figures 6A and 8E). Although the mechanism of this aberrant AEP recruitment is unknown, it indicates that AEP serves an even broader role in MLL leukemogenesis beyond the subset of fusions with AEP components. Determination of whether this role may extend to other MLL fusion proteins requires further investigation. Nevertheless, our studies show that most of the frequently occurring MLL fusions (e.g., MLL-AF4, MLL-AF9, MLL-ENL, and MLL-AF6) use a similar strategy for leukemic transformation, in which AEP is constitutively recruited to MLL target genes either directly or indirectly.

A critical role for AEP in MLL-mediated leukemic transformation suggests that it may be an ideal target for molecular therapy of MLL-associated leukemias. In this regard, our results tentatively support the rationale for CDK9 inhibition as a potential therapeutic strategy, or inhibition of DOT1L whose activity appears to be functionally linked to AEP and possibly plays important roles in the maintenance of the epigenetic status of target genes. However, these molecules are likely to have more generalized roles other than AEP-dependent transcription (Jones et al., 2008; Peterlin and Price, 2006); therefore, serious side effects might occur if they are effectively inhibited. Thus, compounds that specifically target the function of AF4- and ENL family proteins but not P-TEFb or DOT1L may selectively inhibit MLL-dependent transcription and benefit the treatment of MLL-associated leukemias.

EXPERIMENTAL PROCEDURES

Monoclonal Antibodies

Highly specific monoclonal antibodies were generated against MBP fusion proteins containing portions of human AF4 (aa 782–979) (clone 2C.1), human AF5q31 (aa 489–680) (clone 1.3), and human ENL (414–472) (clone 3.1), respectively.

Cell Culture

Human leukemia cell lines K562, HB1119, SEM-K2, KP-L-RY, ML-2, MV4-11, and U937 were cultured in RPMI 1640 medium supplemented with 15% fetal calf serum and nonessential amino acids. MEFs were prepared from E11.5 p53 null embryos. The 293T and plat-E cell lines and MEFs were cultured in Dulbecco's modified Eagle's medium (DMEM) supplemented with 15% fetal calf serum and nonessential amino acids.

Purification of the AEP Complex, Immunoprecipitation, and Western Blotting

The purification procedure for AEP is described in the Supplemental Experimental Procedures. Immunoprecipitation and western blotting methods

are described elsewhere (Yokoyama et al., 2004; 2005). Primary antibodies used in this study are summarized in the Supplemental Experimental Procedures.

Quantitative RT-PCR

Reverse transcription and quantitative PCR were performed as described elsewhere (Yokoyama et al., 2005; Yokoyama and Cleary, 2008) using Taqman probes purchased from Applied Biosystems. The details of the probe set are summarized in the Supplemental Experimental Procedures. Expression levels (average values and standard deviations of triplicate determinations) normalized to housekeeping genes such as *GAPDH* and *β-ACTIN* were calculated using a standard curve and the relative quantification method as described in ABI User Bulletin #2.

Chromatin Immunoprecipitation Assay

Chromatin immunoprecipitations were performed as described elsewhere (Weinmann and Farnham, 2002; Yokoyama and Cleary, 2008). Primary antibodies used in ChIP assays are summarized in Supplemental Experimental Procedures. Quantitative PCR was performed on the precipitated DNAs in triplicate using primers and probes described in Supplemental Experimental Procedures. The values relative to input were determined using a standard curve and the relative quantification method as described in ABI User Bulletin #2.

Vector Construction

cDNA fragments of AF4 and AF5q31 were cloned into pcDNA3.1/*myc*-His A (Invitrogen) for expressing c-*myc* tagged proteins, or pBICEP-CMV-2 (Sigma) for expressing FLAG-tagged proteins. pMSCV-neo constructs encoding MLL-ENL, MLL-AF9, and MLL-AF6 were described elsewhere (Ayton and Cleary, 2003; Somervaille and Cleary, 2006). pMSCV-hygro-Xpress tagged ENL and pMSCV-neo-Xpress tagged MLL-AF5q31-34 were generated by fusing the Xpress-tag sequence from pcDNA4 HisMax vector with the cDNAs of ENL or MLL-AF5q31, respectively. Other expression vectors for various MLL mutants were generated by restriction enzyme digestion or PCR-based mutagenesis. Various FLAG-tagged MLL fusions were also cloned into pCMV5 vector and used for IP analysis. The expression vectors for FLAG-tagged GAL4 fusion proteins were constructed by PCR using pM (Clontech) as template and cloned into pCMV5 vector. The sh-RNA expression vectors targeting murine *Enl* (TRCN0000084405) and human *ENL* (TRCN000019291[#1], TRCN000019293[#2]) were purchased from Open Biosystems.

Virus Production

Ecotropic retrovirus was produced using plat-E packaging cells (Morita et al., 2000). Lentivirus was produced by cotransfection of 293T cells with viral vectors and pCMV dR8.74 and pMD.G packaging constructs (Dull et al., 1998). Supernatant medium containing virus was harvested 48 hr after transfection and was used for transductions.

Myeloid Progenitor Transformation Assay

Myeloid progenitor transformation was assessed as described elsewhere (Lavau et al., 1997; Yokoyama and Cleary, 2008) using cells harvested from the femurs of CD45.1 inbred C57BL/6 mice. C-kit-positive cells were enriched by immunomagnetic selection using an Auto MACS (Miltenyi Biotech), were transduced with recombinant retrovirus by spinoculation, and were plated in methylcellulose medium (M3231, StemCell Technologies) containing SCF, IL-3, IL-6, and GM-CSF. The colony-forming units (CFUs) per 10^4 plated cells were quantified after 5–7 days of culture and were expressed as the average and standard deviation of at least triplicate determinations. For secondary transductions, 10^5 cells were transduced with retrovirus by spinoculation, were cultured in methylcellulose medium overnight, and were selected for drug resistance (hygromycin 750 μg/ml, puromycin 4 μg/ml) for at least 2 days prior to CFC enumeration.

Transactivation Assay

Transactivation assays were performed using 293T cells as described elsewhere (Yokoyama et al., 2002). Cells cultured in 24-well dishes were transfected with 25 ng of pRL-tk, 250 ng of pFR-luc, and 500 ng of pCMV5 FLAG-GAL4 fusion protein vector per well. Cells were lysed 24 hr later and analyzed for luciferase activity using a dual luciferase assay kit according to the manufacturer's instructions (Promega). Relative luciferase activities were normalized to renilla luciferase activities and expressed with the average values and standard deviations of triplicate determinations relative to the GAL4 DNA binding domain controls.

SUPPLEMENTAL INFORMATION

Supplemental information includes five figures and Supplemental Experimental Procedures and may be found with this article online at doi:10.1016/j.ccr.2009.12.040.

ACKNOWLEDGMENTS

We thank Dr. M. Meyerson for providing *Men1* conditional knockout mice, Dr. T. Kitamura for the plat-E cell line, Dr. K. Yamagata for the DOT1L expression vector, and Dr. Y. Zhang for the MLL-DOT1L expression vector. We thank C. Nicolas, M. Ambrus, B. Rouse, C. Hatanaka and M. Kawaguchi, for technical assistance. A.Y. was supported by a Special Fellow Award from the Leukemia and Lymphoma Society. These studies were supported by the Children's Health Initiative of the Packard Foundation and grants from the National Institutes of Health (CA55029 and CA116606) and in part by Grants-in-Aid for Cancer Research (21-6-1) and for the Third-Term Comprehensive 10-Year Strategy for Cancer Control from the Ministry of Health, Labor of Japan.

Received: September 1, 2009
Revised: November 9, 2009
Accepted: December 4, 2009
Published online: February 11, 2010

REFERENCES

Ayton, P.M., and Cleary, M.L. (2003). Transformation of myeloid progenitors by MLL oncoproteins is dependent on Hoxa7 and Hoxa9. Genes Dev. *17*, 2298–2307.

Ayton, P.M., Chen, E.H., and Cleary, M.L. (2004). Binding to nonmethylated CpG DNA is essential for target recognition, transactivation, and myeloid transformation by an MLL oncoprotein. Mol. Cell. Biol. *24*, 10470–10478.

Bitoun, E., Oliver, P.L., and Davies, K.E. (2007). The mixed-lineage leukemia fusion partner AF4 stimulates RNA polymerase II transcriptional elongation and mediates coordinated chromatin remodeling. Hum. Mol. Genet. *16*, 92–106.

Cheung, N., Chan, L.C., Thompson, A., Cleary, M.L., and So, C.W. (2007). Protein arginine-methyltransferase-dependent oncogenesis. Nat. Cell Biol. *9*, 1208–1215.

Collins, E.C., Appert, A., Ariza-McNaughton, L., Pannell, R., Yamada, Y., and Rabbitts, T.H. (2002). Mouse Af9 is a controller of embryo patterning, like Mll, whose human homologue fuses with Af9 after chromosomal translocation in leukemia. Mol. Cell. Biol. *22*, 7313–7324.

Cozzio, A., Passegue, E., Ayton, P.M., Karsunky, H., Cleary, M.L., and Weissman, I.L. (2003). Similar MLL-associated leukemias arising from self-renewing stem cells and short-lived myeloid progenitors. Genes Dev. *17*, 3029–3035.

Daser, A., and Rabbitts, T.H. (2004). Extending the repertoire of the mixed-lineage leukemia gene MLL in leukemogenesis. Genes Dev. *18*, 965–974.

DiMartino, J.F., Miller, T., Ayton, P.M., Landewe, T., Hess, J.L., Cleary, M.L., and Shilatifard, A. (2000). A carboxy-terminal domain of ELL is required and sufficient for immortalization of myeloid progenitors by MLL-ELL. Blood *96*, 3887–3893.

DiMartino, J.F., Ayton, P.M., Chen, E.H., Naftzger, C.C., Young, B.D., and Cleary, M.L. (2002). The AF10 leucine zipper is required for leukemic transformation of myeloid progenitors by MLL-AF10. Blood *99*, 3780–3785.

Domer, P.H., Fakharzadeh, S.S., Chen, C.S., Jockel, J., Johansen, L., Silverman, G.A., Kersey, J.H., and Korsmeyer, S.J. (1993). Acute mixed-lineage leukemia t(4;11)(q21;q23) generates an MLL-AF4 fusion product. Proc. Natl. Acad. Sci. USA *90*, 7884–7888.

Dreyling, M.H., Martinez-Climent, J.A., Zheng, M., Mao, J., Rowley, J.D., and Bohlander, S.K. (1996). The t(10;11)(p13;q14) in the U937 cell line results in the fusion of the AF10 gene and CALM, encoding a new member of the AP-3 clathrin assembly protein family. Proc. Natl. Acad. Sci. USA *93*, 4804–4809.

Dull, T., Zufferey, R., Kelly, M., Mandel, R.J., Nguyen, M., Trono, D., and Naldini, L. (1998). A third-generation lentivirus vector with a conditional packaging system. J. Virol. *72*, 8463–8471.

Erfurth, F., Hemenway, C.S., de Erkenez, A.C., and Domer, P.H. (2004). MLL fusion partners AF4 and AF9 interact at subnuclear foci. Leukemia *18*, 92–102.

Gilliland, D.G. (2002). Molecular genetics of human leukemias: new insights into therapy. Semin. Hematol. *39*, 6–11.

Guenther, M.G., Jenner, R.G., Chevalier, B., Nakamura, T., Croce, C.M., Canaani, E., and Young, R.A. (2005). Global and Hox-specific roles for the MLL1 methyltransferase. Proc. Natl. Acad. Sci. USA *102*, 8603–8608.

Guenther, M.G., Lawton, L.N., Rozovskaia, T., Frampton, G.M., Levine, S.S., Volkert, T.L., Croce, C.M., Nakamura, T., Canaani, E., and Young, R.A. (2008). Aberrant chromatin at genes encoding stem cell regulators in human mixed-lineage leukemia. Genes Dev. *22*, 3403–3408.

Hughes, C.M., Rozenblatt-Rosen, O., Milne, T.A., Copeland, T.D., Levine, S.S., Lee, J.C., Hayes, D.N., Shanmugam, K.S., Bhattacharjee, A., Biondi, C.A., et al. (2004). Menin associates with a trithorax family histone methyltransferase complex and with the hoxc8 locus. Mol. Cell *13*, 587–597.

Huret, J.L., Dessen, P., and Bernheim, A. (2001). An atlas of chromosomes in hematological malignancies. Example: 11q23 and MLL partners. Leukemia *15*, 987–989.

Iida, S., Seto, M., Yamamoto, K., Komatsu, H., Tojo, A., Asano, S., Kamada, N., Ariyoshi, Y., Takahashi, T., and Ueda, R. (1993). MLLT3 gene on 9p22 involved in t(9;11) leukemia encodes a serine/proline rich protein homologous to MLLT1 on 19p13. Oncogene *8*, 3085–3092.

Jansen, M.W., van der Velden, V.H., and van Dongen, J.J. (2005). Efficient and easy detection of MLL-AF4, MLL-AF9 and MLL-ENL fusion gene transcripts by multiplex real-time quantitative RT-PCR in TaqMan and LightCycler. Leukemia *19*, 2016–2018.

Jones, B., Su, H., Bhat, A., Lei, H., Bajko, J., Hevi, S., Baltus, G.A., Kadam, S., Zhai, H., Valdez, R., et al. (2008). The histone H3K79 methyltransferase Dot1L is essential for mammalian development and heterochromatin structure. PLoS Genet. *4*, e1000190. 10.1371/journal.pgen.1000190.

Krivtsov, A.V., and Armstrong, S.A. (2007). MLL translocations, histone modifications and leukaemia stem-cell development. Nat. Rev. Cancer *7*, 823–833.

Krivtsov, A.V., Feng, Z., Lemieux, M.E., Faber, J., Vempati, S., Sinha, A.U., Xia, X., Jesneck, J., Bracken, A.P., Silverman, L.B., et al. (2008). H3K79 methylation profiles define murine and human MLL-AF4 leukemias. Cancer Cell *14*, 355–368.

Lavau, C., Szilvassy, S.J., Slany, R., and Cleary, M.L. (1997). Immortalization and leukemic transformation of a myelomonocytic precursor by retrovirally transduced HRX-ENL. EMBO J. *16*, 4226–4237.

Lavau, C., Du, C., Thirman, M., and Zeleznik-Le, N. (2000). Chromatin-related properties of CBP fused to MLL generate a myelodysplastic-like syndrome that evolves into myeloid leukemia. EMBO J. *19*, 4655–4664.

Li, B., Carey, M., and Workman, J.L. (2007). The role of chromatin during transcription. Cell *128*, 707–719.

Ma, C., and Staudt, L.M. (1996). LAF-4 encodes a lymphoid nuclear protein with transactivation potential that is homologous to AF-4, the gene fused to MLL in t(4;11) leukemias. Blood *87*, 734–745.

McGinty, R.K., Kim, J., Chatterjee, C., Roeder, R.G., and Muir, T.W. (2008). Chemically ubiquitylated histone H2B stimulates hDot1L-mediated intranucleosomal methylation. Nature *453*, 812–816.

Milne, T.A., Briggs, S.D., Brock, H.W., Martin, M.E., Gibbs, D., Allis, C.D., and Hess, J.L. (2002). MLL targets SET domain methyltransferase activity to Hox gene promoters. Mol. Cell *10*, 1107–1117.

Milne, T.A., Hughes, C.M., Lloyd, R., Yang, Z., Rozenblatt-Rosen, O., Dou, Y., Schnepp, R.W., Krankel, C., Livolsi, V.A., Gibbs, D., et al. (2005). Menin and MLL cooperatively regulate expression of cyclin-dependent kinase inhibitors. Proc. Natl. Acad. Sci. USA *102*, 749–754.

Morita, S., Kojima, T., and Kitamura, T. (2000). Plat-E: an efficient and stable system for transient packaging of retroviruses. Gene Ther. *7*, 1063–1066.

Morrissey, J.J., Raney, S., and Cleary, M.L. (1997). The FEL (AF-4) protein donates transcriptional activation sequences to Hrx-Fel fusion proteins in leukemias containing T(4;11)(Q21;Q23) chromosomal translocations. Leuk. Res. *21*, 911–917.

Mueller, D., Bach, C., Zeisig, D., Garcia-Cuellar, M.P., Monroe, S., Sreekumar, A., Zhou, R., Nesvizhskii, A., Chinnaiyan, A., Hess, J.L., and Slany, R.K. (2007). A role for the MLL fusion partner ENL in transcriptional elongation and chromatin modification. Blood *110*, 4445–4454.

Nakamura, T., Alder, H., Gu, Y., Prasad, R., Canaani, O., Kamada, N., Gale, R.P., Lange, B., Crist, W.M., Nowell, P.C., et al. (1993). Genes on chromosomes 4, 9, and 19 involved in 11q23 abnormalities in acute leukemia share sequence homology and/or common motifs. Proc. Natl. Acad. Sci. USA *90*, 4631–4635.

Nakamura, T., Largaespada, D.A., Shaughnessy, J.D., Jr., Jenkins, N.A., and Copeland, N.G. (1996). Cooperative activation of Hoxa and Pbx1-related genes in murine myeloid leukaemias. Nat. Genet. *12*, 149–153.

Nilson, I., Reichel, M., Ennas, M.G., Greim, R., Knorr, C., Siegler, G., Greil, J., Fey, G.H., and Marschalek, R. (1997). Exon/intron structure of the human AF-4 gene, a member of the AF-4/LAF-4/FMR-2 gene family coding for a nuclear protein with structural alterations in acute leukaemia. Br. J. Haematol. *98*, 157–169.

Okada, Y., Feng, Q., Lin, Y., Jiang, Q., Li, Y., Coffield, V.M., Su, L., Xu, G., and Zhang, Y. (2005). hDOT1L links histone methylation to leukemogenesis. Cell *121*, 167–178.

Peterlin, B.M., and Price, D.H. (2006). Controlling the elongation phase of transcription with P-TEFb. Mol. Cell *23*, 297–305.

Prasad, R., Yano, T., Sorio, C., Nakamura, T., Rallapalli, R., Gu, Y., Leshkowitz, D., Croce, C.M., and Canaani, E. (1995). Domains with transcriptional regulatory activity within the ALL1 and AF4 proteins involved in acute leukemia. Proc. Natl. Acad. Sci. USA *92*, 12160–12164.

Pui, C.H., Relling, M.V., and Downing, J.R. (2004). Acute lymphoblastic leukemia. N. Engl. J. Med. *350*, 1535–1548.

Saunders, A., Core, L.J., and Lis, J.T. (2006). Breaking barriers to transcription elongation. Nat. Rev. Mol. Cell Biol. *7*, 557–567.

Slany, R.K., Lavau, C., and Cleary, M.L. (1998). The oncogenic capacity of HRX-ENL requires the transcriptional transactivation activity of ENL and the DNA binding motifs of HRX. Mol. Cell. Biol. *18*, 122–129.

So, C.W., and Cleary, M.L. (2002). MLL-AFX requires the transcriptional effector domains of AFX to transform myeloid progenitors and transdominantly interfere with forkhead protein function. Mol. Cell. Biol. *22*, 6542–6552.

So, C.W., and Cleary, M.L. (2003). Common mechanism for oncogenic activation of MLL by forkhead family proteins. Blood *101*, 633–639.

Somervaille, T.C., and Cleary, M.L. (2006). Identification and characterization of leukemia stem cells in murine MLL-AF9 acute myeloid leukemia. Cancer Cell *10*, 257–268.

Srinivasan, R.S., Nesbit, J.B., Marrero, L., Erfurth, F., LaRussa, V.F., and Hemenway, C.S. (2004). The synthetic peptide PFWT disrupts AF4-AF9 protein complexes and induces apoptosis in t(4;11) leukemia cells. Leukemia *18*, 1364–1372.

Steger, D.J., Lefterova, M.I., Ying, L., Stonestrom, A.J., Schupp, M., Zhuo, D., Vakoc, A.L., Kim, J.E., Chen, J., Lazar, M.A., et al. (2008). DOT1L/KMT4 recruitment and H3K79 methylation are ubiquitously coupled with gene transcription in mammalian cells. Mol. Cell. Biol. *28*, 2825–2839.

Taki, T., Kano, H., Taniwaki, M., Sako, M., Yanagisawa, M., and Hayashi, Y. (1999). AF5q31, a newly identified AF4-related gene, is fused to MLL in infant acute lymphoblastic leukemia with ins(5;11)(q31;q13q23). Proc. Natl. Acad. Sci. USA *96*, 14535–14540.

Tkachuk, D.C., Kohler, S., and Cleary, M.L. (1992). Involvement of a homolog of *Drosophila* trithorax by 11q23 chromosomal translocations in acute leukemias. Cell *71*, 691–700.

von Bergh, A.R., Beverloo, H.B., Rombout, P., van Wering, E.R., van Weel, M.H., Beverstock, G.C., Kluin, P.M., Slater, R.M., and Schuuring, E. (2002).

LAF4, an AF4-related gene, is fused to MLL in infant acute lymphoblastic leukemia. Genes Chromosomes Cancer *35*, 92–96.

Weinmann, A.S., and Farnham, P.J. (2002). Identification of unknown target genes of human transcription factors using chromatin immunoprecipitation. Methods *26*, 37–47.

Wong, P., Iwasaki, M., Somervaille, T.C., So, C.W., and Cleary, M.L. (2007). Meis1 is an essential and rate-limiting regulator of MLL leukemia stem cell potential. Genes Dev. *21*, 2762–2774.

Yokoyama, A., and Cleary, M.L. (2008). Menin critically links MLL proteins with LEDGF on cancer-associated target genes. Cancer Cell *14*, 36–46.

Yokoyama, A., Kitabayashi, I., Ayton, P.M., Cleary, M.L., and Ohki, M. (2002). Leukemia proto-oncoprotein MLL is proteolytically processed into 2 fragments with opposite transcriptional properties. Blood *100*, 3710–3718.

Yokoyama, A., Wang, Z., Wysocka, J., Sanyal, M., Aufiero, D.J., Kitabayashi, I., Herr, W., and Cleary, M.L. (2004). Leukemia proto-oncoprotein MLL forms a SET1-like histone methyltransferase complex with menin to regulate Hox gene expression. Mol. Cell. Biol. *24*, 5639–5649.

Yokoyama, A., Somervaille, T.C., Smith, K.S., Rozenblatt-Rosen, O., Meyerson, M., and Cleary, M.L. (2005). The menin tumor suppressor protein is an essential oncogenic cofactor for MLL-associated leukemogenesis. Cell *123*, 207–218.

Zeisig, D.T., Bittner, C.B., Zeisig, B.B., Garcia-Cuellar, M.P., Hess, J.L., and Slany, R.K. (2005). The eleven-nineteen-leukemia protein ENL connects nuclear MLL fusion partners with chromatin. Oncogene *24*, 5525–5532.

Zhang, W., Xia, X., Reisenauer, M.R., Hemenway, C.S., and Kone, B.C. (2006). Dot1a-AF9 complex mediates histone H3 Lys-79 hypermethylation and repression of ENaCalpha in an aldosterone-sensitive manner. J. Biol. Chem. *281*, 18059–18068.

Published OnlineFirst May 18, 2010; DOI:10.1158/0008-5472.CAN-09-4210

AACR

Cancer Research

Oncostatin M Renders Epithelial Cell Adhesion Molecule–Positive Liver Cancer Stem Cells Sensitive to 5-Fluorouracil by Inducing Hepatocytic Differentiation

Taro Yamashita, Masao Honda, Kouki Nio, et al.

Cancer Res 2010;70:4687-4697. Published OnlineFirst May 18, 2010.

Published OnlineFirst May 18, 2010; DOI:10.1158/0008-5472.CAN-09-4210

Tumor and Stem Cell Biology

Cancer Research

Oncostatin M Renders Epithelial Cell Adhesion Molecule–Positive Liver Cancer Stem Cells Sensitive to 5-Fluorouracil by Inducing Hepatocytic Differentiation

Taro Yamashita, Masao Honda, Kouki Nio, Yasunari Nakamoto, Tatsuya Yamashita, Hiroyuki Takamura, Takashi Tani, Yoh Zen, and Shuichi Kaneko

Abstract

Recent evidence suggests that a certain type of hepatocellular carcinoma (HCC) is hierarchically organized by a subset of cells with stem cell features (cancer stem cells; CSC). Although normal stem cells and CSCs are considered to share similar self-renewal programs, it remains unclear whether differentiation programs are also maintained in CSCs and effectively used for tumor eradication. In this study, we investigated the effect of oncostatin M (OSM), an interleukin 6–related cytokine known to induce the differentiation of hepatoblasts into hepatocytes, on liver CSCs. OSM receptor expression was detected in the majority of epithelial cell adhesion molecule–positive ($EpCAM^+$) HCC with stem/progenitor cell features. OSM treatment resulted in the induction of hepatocytic differentiation of $EpCAM^+$ HCC cells by inducing signal transducer and activator of transcription 3 activation, as determined by a decrease in stemness-related gene expression, a decrease in EpCAM, α-fetoprotein and cytokeratin 19 protein expressions, and an increase in albumin protein expression. OSM-treated $EpCAM^+$ HCC cells showed enhanced cell proliferation with expansion of the EpCAM-negative non-CSC population. Noticeably, combination of OSM treatment with the chemotherapeutic agent 5-fluorouracil (5-FU), which eradicates EpCAM-negative non-CSCs, dramatically increased the number of apoptotic cells *in vitro* and suppressed tumor growth *in vivo* compared with either saline control, OSM, or 5-FU treatment alone. Taken together, our data suggest that OSM could be effectively used for the differentiation and active cell division of dormant $EpCAM^+$ liver CSCs, and the combination of OSM and conventional chemotherapy with 5-FU efficiently eliminates HCC by targeting both CSCs and non-CSCs. *Cancer Res; 70(11); 4687–97. ©2010 AACR.*

Introduction

It is widely accepted that cancer is a disease that develops from a normal cell with accumulated genetic/epigenetic changes. Although considered monoclonal in origin, cancer is composed of heterogeneous cellular populations. These heterogeneities are traditionally explained by the clonal evolution of cancer cells through a series of stochastic genetic events (clonal evolution model; ref. 1). In contrast, cancer cells are known to have the capabilities characteristic of stem cells with respect to self-renewal, limitless division, and generation of heterogeneous cell populations. Recent evidence suggests that tumor cells possess stem cell features (cancer stem cells; CSC) to self-renew and give rise to relatively differentiated cells through asymmetric division, and thereby form heterogeneous populations (CSC model; refs. 2, 3). Accumulating evidence supports the notion that CSCs could generate tumors more efficiently in immunodeficient mice than non-CSCs in the case of leukemia and various solid tumors (4–9), although the origin of CSCs is still a controversial issue.

Worldwide, hepatocellular carcinoma (HCC) is one of the most common malignancies with poor outcome (10). Recent evidence suggests that at least some HCCs are organized by liver CSCs in a hierarchical manner (11). Several markers have been identified as useful for the enrichment of liver CSCs, including side population fraction (12), CD133 (13), CD90 (14), and OV6 (15). We have recently used epithelial cell adhesion molecule (EpCAM) and α-fetoprotein (AFP) to identify novel prognostic HCC subtypes related to certain developmental stages of human liver lineages (16). Among these, EpCAM-positive ($^+$) AFP^+ HCC (hepatic stem cell–like HCC) is characterized by young onset of disease, activation of Wnt/β-catenin signaling, and poor prognosis. *EPCAM* is a target gene of Wnt/β-catenin signaling (17), and we previously identified that $EpCAM^+$ HCC cells from primary HCC

Authors' Affiliation: Center for Liver Diseases, Kanazawa University Hospital, Kanazawa, Ishikawa, Japan

Note: Supplementary data for this article are available at Cancer Research Online (http://cancerres.aacrjournals.org/).

Corresponding Authors: Taro Yamashita, Department of Gastroenterology, Kanazawa University Graduate School of Medical Science, 13-1 Takara-Machi, Kanazawa, Ishikawa 920-8641, Japan. Phone: 81-76-265-2851; Fax: 81-76-265-4250; E-mail: taroy@m-kanazawa.jp and Shuichi Kaneko, Center for Liver Diseases, Kanazawa University Hospital; Department of Gastroenterology, Kanazawa University Graduate School of Medical Science, 13-1 Takara-Machi, Kanazawa, Ishikawa 920-8641, Japan. Phone: 81-76-265-2230; Fax: 81-76-265-4250; E-mail: skaneko@m-kanazawa.jp.

doi: 10.1158/0008-5472.CAN-09-4210

Published OnlineFirst May 18, 2010; DOI:10.1158/0008-5472.CAN-09-4210

samples and cell lines have the features of CSCs, at least in the hepatic stem cell–like HCC subtype (18). Thus, EpCAM seems to be a potentially useful marker for the isolation of liver CSCs in hepatic stem cell–like HCC.

CSCs are considered to be resistant to chemotherapy and radiotherapy (19–21), which may be associated with the recurrence of the tumor after treatment. These findings have led to the proposal of "destemming" CSCs, to induce the differentiation of CSCs into non-CSCs or to eradicate CSCs by inhibiting the signaling pathway responsible for self-renewal (22). Recent studies support this proposal and suggest the utility of bone morphogenetic proteins, activated during embryogenesis and required for differentiation of neuronal stem cells, to induce differentiation of brain CSCs and facilitate brain tumor eradication (23, 24). However, it is still debatable whether simple differentiation of CSCs effectively eradicates tumors (25).

Oncostatin M (OSM), an interleukin (IL)-6–related cytokine produced by $CD45^+$ hematopoietic cells, is known to enhance hepatocytic differentiation of hepatoblasts by inducing the activation of the signal transducer and activator of transcription 3 (STAT3) pathway (26). Although OSM, IL-6, and leukemia-inhibitory factor share STAT3 signaling cascades, OSM is known to exploit the distinct hepatocytic differentiation signaling in an OSM receptor (OSMR)–specific manner (27). In this study, we hypothesized that OSM induces hepatocytic differentiation of liver CSCs through the OSMR signaling pathway. We examined OSMR expression and the effect of OSM in $EpCAM^+$ HCC in terms of hepatocytic differentiation and antitumor activities.

Materials and Methods

Clinical HCC specimens

A total of 107 HCC tissues and adjacent noncancerous liver tissues were obtained from patients who underwent hepatectomy for HCC treatment from 1999 to 2007 in Kanazawa University Hospital. These samples were formalin-fixed and paraffin-embedded, and used for immunohistochemistry. HCC and adjacent noncancerous liver tissues were histologically diagnosed by two pathologists. An additional fresh $EpCAM^+$ AFP^+ HCC sample was obtained from a surgically resected specimen and immediately used for the preparation of single-cell suspensions and xenotransplantation. All tissue acquisition procedures were approved by the Ethics Committee and the Institutional Review Board of Kanazawa University Hospital. All patients provided written informed consent.

Cell culture and reagents

HuH1 and HuH7 cells were cultured as previously described (18). A primary HCC tissue was dissected and digested in 1 μg/mL of type 4 collagenase (Sigma-Aldrich Japan K.K.) solution at 37°C for 15 to 30 minutes. Contaminated RBC were lysed with ammonium chloride solution (STEMCELL Technologies) on ice for 5 minutes. $CD45^+$ leukocytes and Annexin V^+ apoptotic cells were removed by autoMACS-pro cell separator and magnet beads (Miltenyi Biotec K.K.). EpCAM-positive and -negative cells were enriched by autoMACS-pro cell separator and CD326 (EpCAM) MicroBeads (Miltenyi Biotec K.K.). Recombinant OSM was purchased from R&D Systems, Inc. 5-Fluorouracil (5-FU) was obtained from Kyowa Kirin.

Quantitative reverse transcription-PCR analysis

Total RNA was extracted using TRIzol (Invitrogen) according to the instructions of the manufacturer. The expression of selected genes was determined in triplicate using the 7900 Sequence Detection System (Applied Biosystems). Each sample was normalized relative to β-actin expression. Probes used were *TACSTD1*, Hs00158980_m1; *AFP*, Hs00173490_m1; *KRT19*, Hs00761767_s1; *hTERT*, Hs00162669_m1; *Bmi1*, Hs00180411_m1; *POU5F1*, Hs00999632_g1; *CYP3A4*, Hs00430021_m1; *OSMR*, Hs00384278_m1; and *ACTB*, Hs99999903_m1 (Applied Biosystems).

Western blotting

Whole cell lysates were prepared using radioimmunoprecipitation assay lysis buffer as described previously (28). Rabbit polyclonal antibodies to STAT3 (Cell Signaling Technology, Inc.), rabbit polyclonal anti-OSMR antibodies H-200 (Santa Cruz Biotechnology), mouse monoclonal anti–phosphorylated STAT3 (Tyr^{705}) antibody (3E2; Cell Signaling Technology), and mouse monoclonal anti–β-actin antibody (Sigma-Aldrich) were used. Immune complexes were visualized by enhanced chemiluminescence (Amersham Biosciences, Corp.) as described by the manufacturer.

Immunohistochemistry and immunofluorescence analyses

Immunohistochemistry was performed using Envision+ kits (DAKO) according to the instructions of the manufacturer. Anti-EpCAM monoclonal antibody, VU-1D9 (Oncogene Research Products), was used for detecting EpCAM. Goat anti-OSMR polyclonal antibodies (C-20) were obtained from Santa Cruz Biotechnology. Mouse anti-CYP3A4 polyclonal antibodies (Abnova), mouse anti–cytokeratin (CK) 19 monoclonal antibody (DAKO), and mouse anti–Ki-67 monoclonal antibody MIB-1 (DAKO) were used for detecting CYP3A4, CK19, and Ki-67, respectively. Samples with >5% positive staining in a given area for a particular antibody were considered to be positive. For immunofluorescence analyses, anti-EpCAM antibody (Oncogene Research Products), anti-gp130ST antibodies (Santa Cruz Biotechnology), and anti–phosphorylated STAT3 (Tyr^{705}) antibody (3E2; Cell Signaling Technology) were used. Alexa 488 FITC-conjugated anti-mouse IgG or Alexa 568 Texas red–conjugated anti-goat/rabbit IgG (Molecular Probes) were used as secondary antibodies. Confocal fluorescence microscopic analysis was performed essentially as previously described (18).

Fluorescence-activated cell sorting analyses

Cultured cells were trypsinized, washed, and resuspended in HBSS (Lonza) supplemented with 1% HEPES and 2% fetal bovine serum (FBS). Cells were then incubated with FITC-conjugated anti-EpCAM monoclonal antibody Clone Ber-EP4 (DAKO) on ice for 30 minutes, and analyzed using

Published OnlineFirst May 18, 2010; DOI:10.1158/0008-5472.CAN-09-4210

a FACSCalibur (BD Biosciences). Intracellular AFP, CK19, and albumin levels were examined using a BD Cytofix/Cytoperm Fixation/Permeabilization Kit (BD Biosciences), anti-AFP mouse monoclonal antibody (Nichirei Biosciences Inc.), anti-CK19 mouse monoclonal antibody (DAKO), and rabbit polyclonal anti-albumin antibodies (Cell Signaling Technology), respectively.

Cell proliferation and colony formation assay

For cell proliferation assays, 2×10^3 cells were seeded in 96-well plates and cultured with 1% FBS DMEM (control), 1% DMEM with OSM (100 ng/mL), 5-FU (2 μg/mL), or OSM (100 ng/mL) and 5-FU (2 μg/mL) for 3 to 7 days without media changes. Cell viability was evaluated in quadruplicate using a CellTiter 96 AQueous kit (Promega). For colony formation assays, 1×10^3 cells were harvested in a one-well Culture Slide (BD Biosciences) and cultured with 1% FBS DMEM (control) with or without OSM (100 ng/mL). Culture medium was replaced every 3 days and the colonies were fixed with ice-cold 100% methanol and used for immunofluorescence 10 days after the initiation of treatment.

RNA interference

SiRNAs specific to OSMR (Silencer Select siRNA S17542) and a control siRNA (Silencer Select Negative Control no. 1) were obtained from Ambion (Applied Biosystems). To each well of a six-well plate, 2×10^5 cells were seeded 12 hours before transfection. Transfection was performed using LipofectAMINE 2000 (Invitrogen), according to the instructions of the manufacturer. A total of 100 pmol/L of siRNA duplex was used for each transfection.

Apoptosis assay

Cells were cultured in 1% FBS DMEM (control), 1% FBS DMEM with OSM (100 ng/mL), 5-FU (2 μg/mL), or OSM (100 ng/mL) and 5-FU (2 μg/mL) for 3 days in six-well plates or in culture slides (BD Biosciences). Annexin V binding to cell membranes was visualized using Annexin V-FITC antibodies and a FACSCalibur flow cytometer (BD Biosciences). Activation of caspase 3 was visualized by immunohistochemistry or immunofluorescence using anti-active caspase-3 polyclonal antibodies (Promega), as described by the manufacturer.

Animal studies

Six-week-old NOD/SCID mice (NOD/NCrCRl-*Prkdc*^{scid}) were purchased from Charles River Laboratories, Inc. The protocol was approved by the Kanazawa University Animal Care and Use Committee. One million tumor cells were suspended in 200 μL of DMEM and Matrigel (1:1), and a s.c. injection was performed. The incidence and size of subcutaneous tumors were recorded. Intratumoral injections of 50 μL of PBS (control), OSM (2 μg/tumor), 5-FU (250 μg/tumor), or OSM (2 μg/tumor) and 5-FU (250 μg/tumor) were initiated twice weekly 48 days after the injection of tumor cells when the average volume of four tumors in each group had reached 400 mm^3. For histologic evaluation, tumors were formalin-fixed and paraffin-embedded.

Statistical analyses

The association of OSMR expression and clinicopathologic characteristics in HCC was examined using either Mann-Whitney U or χ^2 tests. Student's t test was used to compare various test groups assayed by quantitative reverse transcription-PCR analysis. All analyses were performed using GraphPad Prism software.

Results

Distinct expression of OSMRs in HCC

Before exploring the effect of OSM on HCC, we examined the expression of its receptor, OSMR, in surgically resected HCC and adjacent noncancerous liver tissues by immunohistochemistry. Representative staining of OSMRs in tumor/nontumor tissues is shown in Fig. 1A. In general, cell surface and cytoplasmic immunoreactivity to OSMR were rarely detected in hepatocytes in chronic hepatitis liver (a), but were frequently detected in small hepatocyte-like cells in the stroma or transitional cells in the lobule of cirrhotic liver (b), as indicated by the arrows. Note that immunoreactivity to OSMR was not detected in bile duct epithelia or ductular reactions in which EpCAM$^+$ hepatic progenitor cells are thought to accumulate (Supplementary Fig. S1), suggesting that OSMRs might be expressed in hepatic progenitor cells committed to hepatocytes. Immunoreactivity to OSMRs was more strongly detected in HCC than in noncancerous liver (c), and the expression was heterogeneous in the tumor. Of note, OSMRs were detected in HCC cells at the invasive front area of the tumor (d) where CSCs are known to invade frequently (arrows).

Immunoreactivity to OSMR antibodies and EpCAM antibodies was detected in 66 (61.7%) and 38 (35.5%) of 107 HCC specimens, respectively. The clinicopathologic characteristics of OSMR$^+$ and OSMR$^-$ HCC cases are shown in Table 1. OSMR$^+$ HCC was characterized by high serum AFP values ($P = 0.009$), poorly differentiated morphology ($P < 0.0001$), and a high frequency of EpCAM$^+$ HCCs ($P = 0.024$), suggesting that the OSMR is expressed in HCC with stem/progenitor cell features. OSMR$^+$ HCC was also characterized by young onset of disease and male dominance, although these features did not reach statistical significance ($P = 0.052$ and 0.058, respectively). OSMR was more frequently detected in EpCAM$^+$ HCCs (76.3%) than in EpCAM$^-$ HCCs (53.7%). Expression of OSMR and EpCAM was further investigated by double immunofluorescence analysis, and immunoreactivity to OSMR was detected in both EpCAM$^+$ normal hepatic progenitors (Fig. 1B) and EpCAM$^+$ HCC cells (Fig. 1C). These data suggest that although OSMR is more widely expressed than EpCAM in HCC, OSMR is frequently expressed in EpCAM$^+$ normal hepatic progenitors and liver CSCs.

OSM induces hepatocytic differentiation of EpCAM+ HCC

Because OSMR was expressed in the majority of EpCAM$^+$ HCCs, we investigated the effect of OSM on EpCAM$^+$ HCC cell lines. First, we examined the expression of OSMR and its signal transducer glycoprotein 130 (gp130) in EpCAM$^+$ AFP$^+$ HCC cell lines HuH1 and HuH7 by immunofluorescence

Published OnlineFirst May 18, 2010; DOI:10.1158/0008-5472.CAN-09-4210

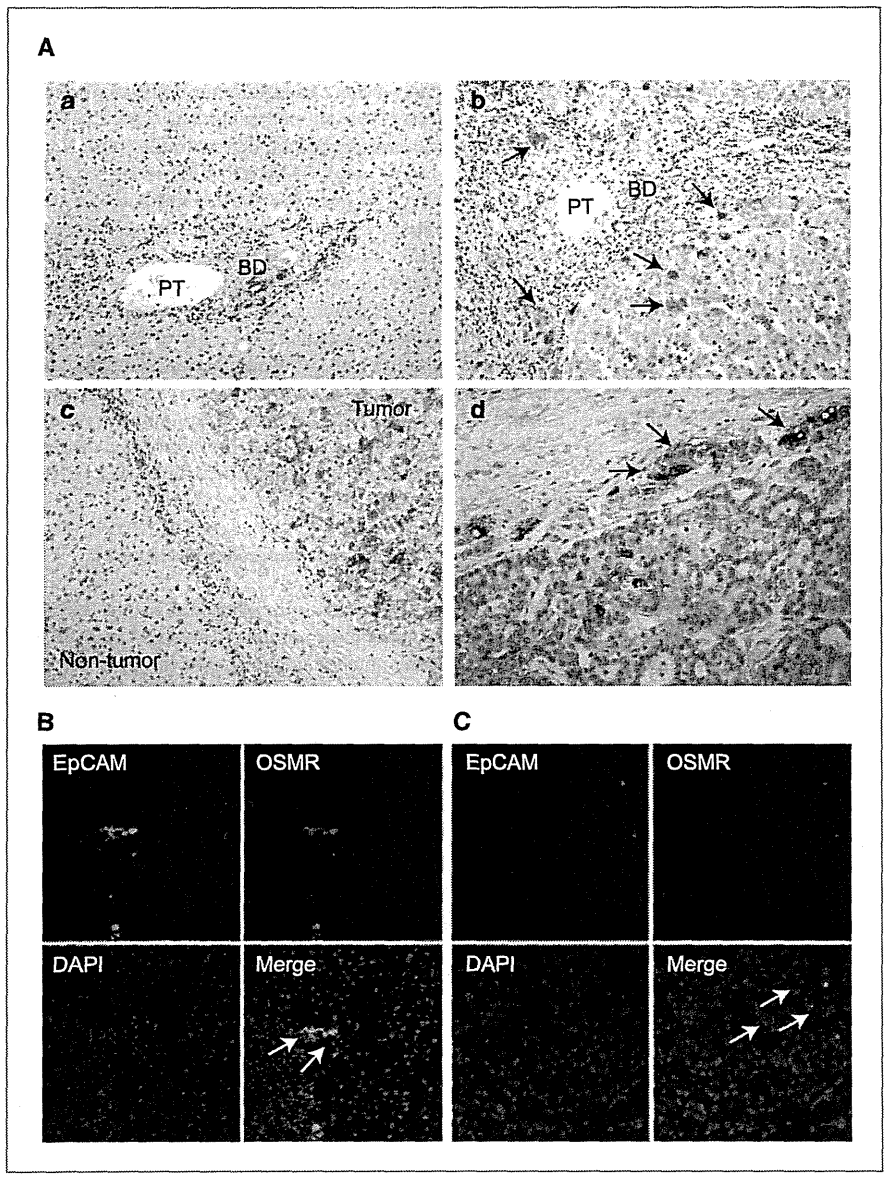

Figure 1. A, representative images of OSMR staining in noncancerous liver tissues and HCC tissues. Immunoreactivity to OSMR was not detected in hepatocytes in chronic hepatitis liver tissue (a) but was detected in a subset of small hepatocyte-like cells in the stroma or transitional cells in the lobule (b, arrows) of cirrhotic liver tissue. OSMR was more abundantly expressed in HCC than in noncancerous liver (c). OSMR$^+$ cancer cells were disseminated in the invasive front area of the tumor (d, arrows). PT, portal tract; BD, bile duct. B and C, double immunofluorescence analysis of EpCAM (green) and OSMR (red) expression in noncancerous (B) and HCC (C) tissues.

(Fig. 2A). Both gp130 and OSMR protein expressions were detected in these cells, consistent with the immunohistochemical data. Because OSM is known to induce the hepatocytic differentiation of hepatoblasts in a STAT3-dependent manner, we investigated the effect of OSM on phosphorylation of STAT3 in HuH1 and HuH7 cells by immunofluorescence and Western blotting. Incubation of HCC cells for 1 hour with OSM at a concentration of 100 ng/mL resulted in the induction and nuclear accumulation of phosphorylated STAT3 compared with controls (Fig. 2B and C). We examined the effect of OSM on the EpCAM$^+$ cell population in HuH1 and HuH7 cells. We first labeled HuH1 and HuH7 cells with CD326 (EpCAM) MicroBeads and FITC-conjugated anti-EpCAM antibodies (Clone Ber-EP4) and performed positive/negative selection using magnetic activated cell sorting to determine the appropriate gating criteria for EpCAM-high (designated as EpCAM$^+$) and EpCAM-low/negative (designated as EpCAM$^-$) cell population (Fig. 2D, top). It is interesting that OSM treatment (100 ng/mL for 72 hours) diminished the EpCAM$^+$ cell population from 50.7% to 10.1% in HuH1 and from 55.2% to 28.8% in HuH7 cells when the same constant gating criteria was applied (Fig. 2D, bottom).

We used RNA interference to investigate whether the decrease in EpCAM$^+$ cells by OSM treatment depends on the expression of OSMR. Transfection of siRNAs specific to *OSMR* (si-OSMR) resulted in the knockdown of target genes

Published OnlineFirst May 18, 2010; DOI:10.1158/0008-5472.CAN-09-4210

compared with the control (si-Control) in HuH1 and HuH7 cells 48 hours after transfection (Supplementary Fig. S2A). We further confirmed the decrease of OSMR protein expression by immunofluorescence and Western blotting 72 hours after transfection (Supplementary Fig. S2B and C). When we treated these HuH1 and HuH7 cells with OSM (100 ng/mL) for 1 hour, we observed the decrease of phosphorylated STAT3 by *OSMR* gene silencing compared with the control (Supplementary Fig. S2C). Furthermore, OSM-mediated decrease in the number of EpCAM$^+$ cells was inhibited by *OSMR* gene silencing (Supplementary Fig. S2D), suggesting that OSM exploits the diminution of EpCAM$^+$ cells through the activation of the OSMR signaling pathway in EpCAM$^+$ HCC.

We further examined the effect of OSM on hepatocytic differentiation by quantitative reverse transcription-PCR and fluorescence-activated cell sorting (FACS) analyses. OSM treatment in HuH1 cells reduced the expression of hepatic progenitor–related genes including *AFP, KRT19* (encoding CK19), and *TERT* (encoding telomerase reverse transcriptase; TERT; Fig. 3A). OSM treatment further reduced the expression of *BMI1* and *POU5F1* (encoding Oct4), which is known to be expressed and required for self-renewal in embryonic stem cells. OSM treatment also increased the expression of the hepatocyte marker, *CYP3A4*. Furthermore, OSM treatment reduced AFP$^+$ and CK19$^+$ cells and increased albumin$^+$ cells compared with the untreated controls, as evaluated by the geometric mean of the fluorescence intensities of whole cells analyzed by intracellular FACS (Fig. 3B). Similar results were obtained in HuH7 cells (data not shown) and, taken together, these data suggest that OSM induced the hepatocytic differentiation of EpCAM$^+$ HCCs.

Hepatocytic differentiation of EpCAM+ HCC by OSM augments cell proliferation

In general, normal stem cells are more quiescent than differentiated cells in terms of cell division. We therefore evaluated the effect of OSM on cell proliferation in HuH1 and HuH7 cells. It is interesting that OSM treatment for 10 days resulted in a larger colony formation following treatment with OSM (100 ng/mL) compared with untreated controls. Of note, the majority of cells comprising these larger colonies were EpCAM$^-$, or had low expression levels, whereas a subset of untreated control cells maintained high EpCAM expression (Fig. 3C). Similar results were obtained when cell proliferation was examined using a [3-(4, 5-dimethylthiazol-2-yl)-5-(3-carboxymethoxyphenyl)-2-(4-sulfophenyl)-2H-tetrazolium] tetrazolium assay and Ki-67 labeling index (Fig. 3D). OSM modestly enhanced cell proliferation (top) and increased Ki-67–positive cells (middle and bottom) compared with untreated controls in both HuH1 and HuH7 cells with statistical significance (Fig. 3D).

OSM treatment increases chemosensitivity of EpCAM+ HCC

The abovementioned data imply that although OSM may induce the hepatocytic differentiation of dormant EpCAM$^+$ liver CSCs, OSM treatment alone might instead enhance cell proliferation through expansion of amplifying differentiated cancer cells *in vitro*, raising the question of efficacy of differentiation therapy in EpCAM$^+$ HCC. Because rapidly amplifying cells are considered to be more sensitive to chemotherapeutic agents, we investigated the effect of combining OSM treatment with conventional chemotherapy to target both dormant CSCs and amplifying non-CSCs. We have shown that 5-FU treatment

Table 1. Clinicopathologic characteristics of OSMR$^+$ and OSMR$^-$ HCC cases used for immunohistochemical analyses

Variables	OSMR$^+$ (n = 66)	OSMR$^-$ (n = 41)	P*
Age (years, mean ± SE)	62.7 ± 1.3	66.4 ± 1.3	0.052
Sex (male/female)	55/11	27/14	0.058
Etiology (HBV/HCV/other)	25/35/6	8/30/3	0.10
Liver cirrhosis (yes/no)	43/23	26/15	1.0
AFP (ng/mL, mean ± SE)	6,453 ± 5901	1,039 ± 935	0.009
Histologic grade†			
I–II	3	16	
II–III	54	20	
III–IV	9	5	<0.0001
Tumor size (<3 cm/>3 cm)	30/36	15/26	0.42
Tumor-node-metastasis classification			
I/II	48	31	
III/IV	18	10	0.82
EpCAM (positive/negative)	29/37	9/32	0.024

*Mann-Whitney U test or χ^2 test.
†Edmondson-Steiner.

Published OnlineFirst May 18, 2010; DOI:10.1158/0008-5472.CAN-09-4210

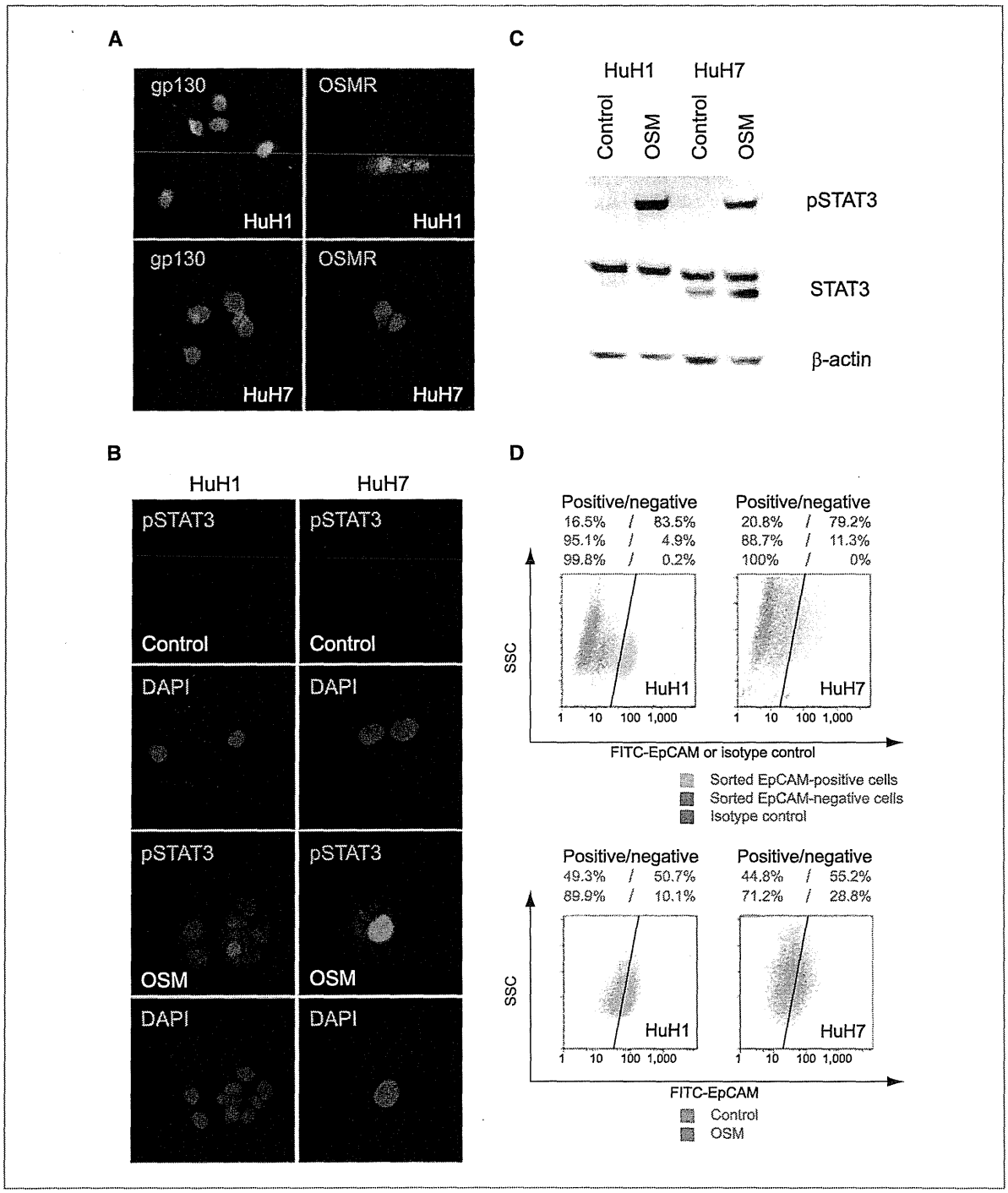

Figure 2. A, immunofluorescence analysis of gp130 and OSMR expression in HuH1 and HuH7 cell lines. B, immunofluorescence analysis of phosphorylated STAT3 expression in HuH1 and HuH7 cell lines stimulated by OSM (100 ng/mL for 1 hour) and controls. C, Western blotting analysis of whole or phosphorylated STAT3 protein expression in HuH1 and HuH7 cells stimulated by OSM (100 ng/mL for 1 hour) and controls. D, FACS analysis of HuH1 and HuH7 cells stained with FITC-conjugated anti-EpCAM antibodies. Top, EpCAM-high (designated as $EpCAM^+$; yellow) and EpCAM-low/negative cells (designated as $EpCAM^-$; blue) were enriched by magnetic activated cell sorting and labeled with FITC-conjugated anti-EpCAM antibodies or isotype control antibodies. Bottom, cells were cultured in 1% FBS DMEM with (green) or without OSM (100 ng/mL; orange) for 3 days and stained with FITC-conjugated anti-EpCAM antibodies.

Published OnlineFirst May 18, 2010; DOI:10.1158/0008-5472.CAN-09-4210

alone could diminish EpCAM⁻ non-CSCs which results in the enrichment of EpCAM⁺ CSCs in HCC (18). We therefore explored the effect of 5-FU in combination with OSM on EpCAM⁺ HCC cell proliferation and apoptosis *in vitro*.

When HuH1 and HuH7 cells were treated with OSM alone and cultured for 7 days, cell proliferation was modestly increased compared with untreated controls (Fig. 4A). In contrast, 5-FU treatment clearly inhibited cell proliferation.

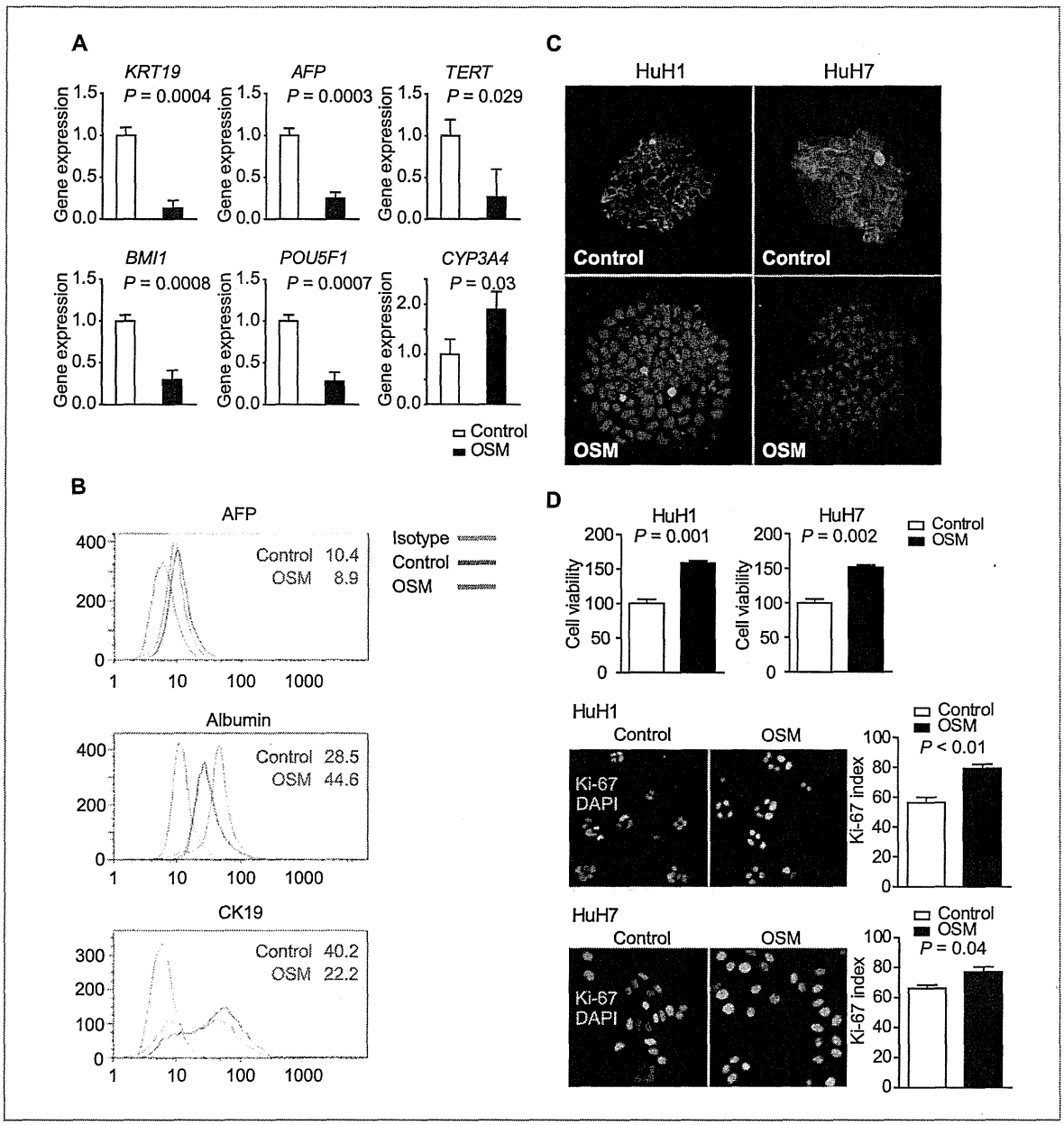

Figure 3. A, quantitative reverse transcription-PCR analysis of HuH1 cells cultured in 1% FBS DMEM with (black columns) or without (white columns) OSM (100 ng/mL) for 3 days. B, intracellular FACS analysis of HuH1 cells cultured in 1% FBS DMEM with (green line) or without (red line) OSM (100 ng/mL) for 3 days. The number in the figure indicates the geometric mean of the fluorescence intensity on a logarithmic scale. C, immunofluorescence analysis of HuH1 and HuH7 cell colonies cultured in 1% FBS DMEM with or without OSM (100 ng/mL) for 10 days. Colonies were fixed with 100% ice-cold methanol and stained with FITC-conjugated anti-EpCAM antibodies. D, top, cell proliferation assay of HuH1 and HuH7 cells cultured in 1% FBS DMEM with (black column) or without (white column) OSM (100 ng/mL) for 3 days. Middle and bottom, immunofluorescence analysis of HuH1 and HuH7 cells cultured in 1% FBS DMEM with or without OSM (100 ng/mL) for 3 days. Cells were fixed with 100% ice-cold methanol and stained with anti–Ki-67 antibodies.

Published OnlineFirst May 18, 2010; DOI:10.1158/0008-5472.CAN-09-4210

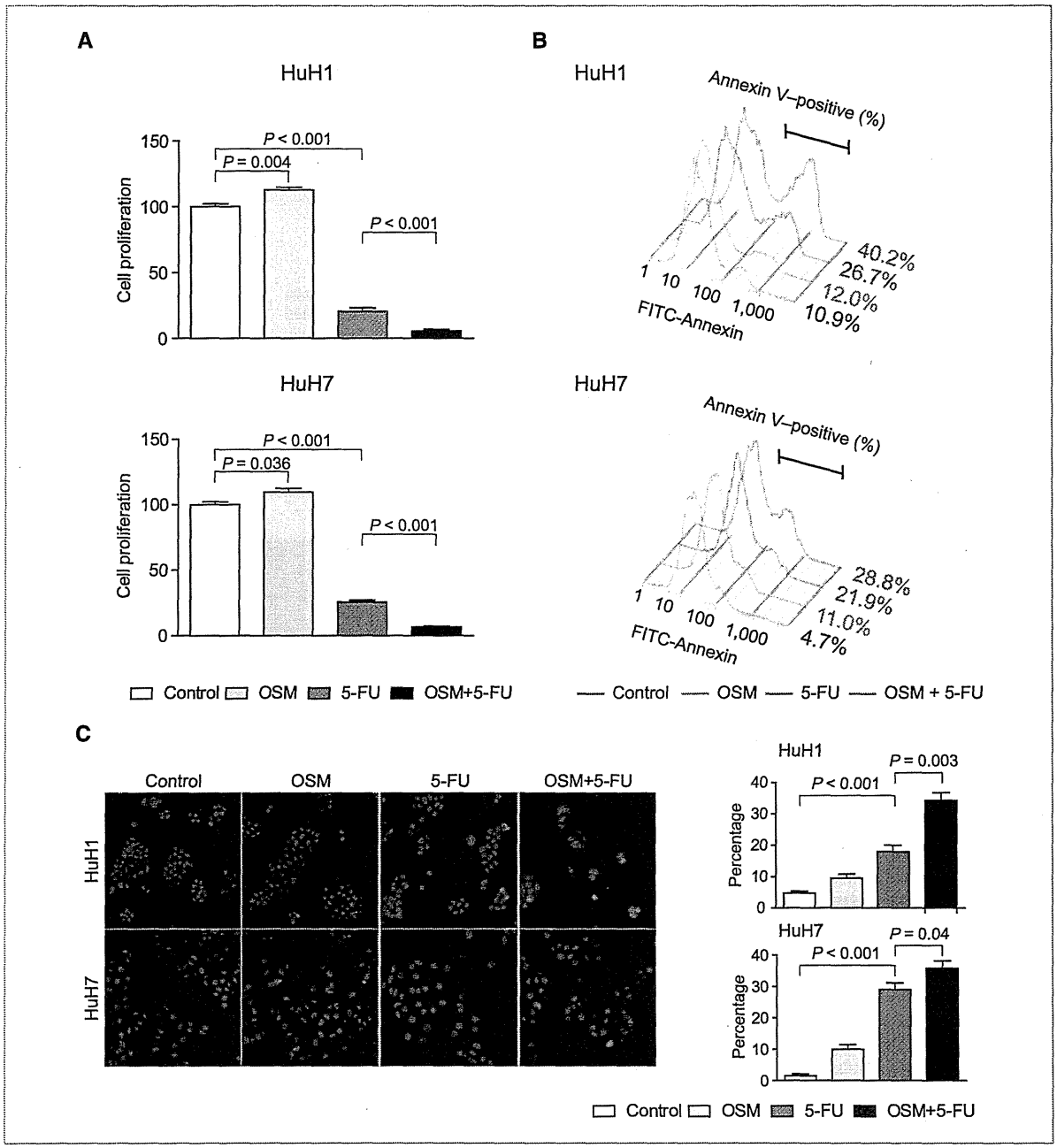

Figure 4. A, cell proliferation assay of HuH1 and HuH7 cells cultured in 1% FBS DMEM with OSM (100 ng/mL; light gray columns), 5-FU (2 μg/mL; gray columns), OSM (100 ng/mL) and 5-FU (2 μg/mL; black columns), or PBS as control (white columns) for 7 days. B, FACS analysis of HuH1 and HuH7 cells stained with FITC-conjugated anti–Annexin V antibodies. Cells were cultured in 1% FBS DMEM with OSM (100 ng/mL; green line), 5-FU (2 μg/mL; blue line), OSM (100 ng/mL) and 5-FU (2 μg/mL; red line), or PBS as control (gray line) for 3 days. C, left, immunofluorescence analysis of HuH1 and HuH7 cells stained with anti–active caspase 3 antibodies. Cells were cultured in 1% FBS DMEM with OSM (100 ng/mL), 5-FU (2 μg/mL), OSM (100 ng/mL) and 5-FU (2 μg/mL), or PBS control for 3 days. Right, bar graphs indicating the percentages of active caspase 3–positive cells.

Noticeably, the combination of OSM and 5-FU effectively suppressed cell proliferation in HuH1 and HuH7 cells (Fig. 4A). We further investigated the effects of OSM and 5-FU on apoptosis, evaluated by Annexin V binding to cell membranes and the activation of caspase 3 (Fig. 4B and C). Although OSM treatment alone had a small effect on the induction of apoptosis, 5-FU treatment induced Annexin V^+ and activated caspase 3^+ cells more than in the control. The

Published OnlineFirst May 18, 2010; DOI:10.1158/0008-5472.CAN-09-4210

combination of OSM and 5-FU most strongly induced apoptosis in both HuH1 and HuH7 cells with statistical significance.

Finally, we investigated the effect of OSM on EpCAM+ HCC *in vivo* using a primary HCC specimen and cell lines. Single-cell suspensions from primary EpCAM+ HCC cells (1×10^6 cells) were injected into 6-week-old male NOD/SCID mice, and these cells formed subcutaneous tumors 48 days after transplantation. Subsequently, 50 μL of PBS, OSM (2 μg/tumor), 5-FU (250 μg/tumor), or OSM (2 μg/tumor) and 5-FU (250 μg/tumor) solution were injected directly into each tumor twice a week. Although OSM treatment alone showed weak tumor-suppressive effects, the changes in tumor size showed no significant difference compared with controls (Fig. 5A). Similarly, 5-FU treatment alone showed limited tumor-suppressive effects. However, the combination of OSM with 5-FU showed a marked inhibition of tumor growth compared with PBS control or 5-FU alone (P = 0.02 and 0.05, respectively). Immunohistochemical analysis of xenografted tumors showed that OSM treatment decreased the number of EpCAM+ or CK19+ cells and increased CYP3A4+ cells *in vivo* (Supplementary Fig. S3A and B). FACS analysis of xenografted tumors further confirmed the decrease of EpCAM+ cell population by OSM treatment *in vivo* (Supplementary Fig. S3C). Immunohistochemical analysis revealed that the combination of OSM with 5-FU strongly induced the activation of caspase 3 compared with PBS control, OSM, or 5-FU (Fig. 5B). Taken together, these data suggest that hepatocytic differentiation of EpCAM+ HCC cells induced by OSM was the most effective for inhibition of tumor growth *in vivo* when the conventional chemotherapeutic agent 5-FU was coadministered.

Discussion

A growing body of evidence suggests that there are similarities between normal stem cells and CSCs in terms of self-renewal programs (29). We have recently reported that Wnt/β-catenin signaling augments self-renewal and inhibits the differentiation of EpCAM+ liver CSCs (18). In the present study, we have shown that the OSM-OSMR signaling pathway is maintained in HCCs with stem/progenitor cell features. OSM induces hepatocytic differentiation and activates cell division in dormant EpCAM+ liver CSCs (Fig. 5C). Furthermore, we have shown that the combination of OSM and 5-FU effectively inhibits tumor cell growth, revealing the importance of targeting both CSCs and non-CSCs for eradication of the tumor.

OSM is a pleiotropic cytokine that belongs to the IL-6 family which includes IL-6, IL-11, and leukemia-inhibitory factor. These cytokines share the gp130 receptor subunit as a common signal transducer, and activate Janus tyrosine kinases and the STAT3 pathway. However, gp130 forms a heterodimer with a unique partner such as the IL-6 receptor, leukemia-inhibitory factor receptor, or OSMR, thus transducing a certain signaling uniquely induced by each cytokine (30). Of note, OSM is known to activate hepatocytic differentiation programs in hepatoblasts in an OSMR-specific manner (27), and our data showed that OSM could induce hepatocytic differentiation and active cell proliferation in EpCAM+ HCC through OSMR signaling.

OSMR is expressed in hepatoblasts in the fetal liver (26). We have found that OSMR is frequently expressed in normal hepatic progenitors but is rarely detected in hepatocytes in adult livers. Interestingly, OSMR+ HCC was characterized by

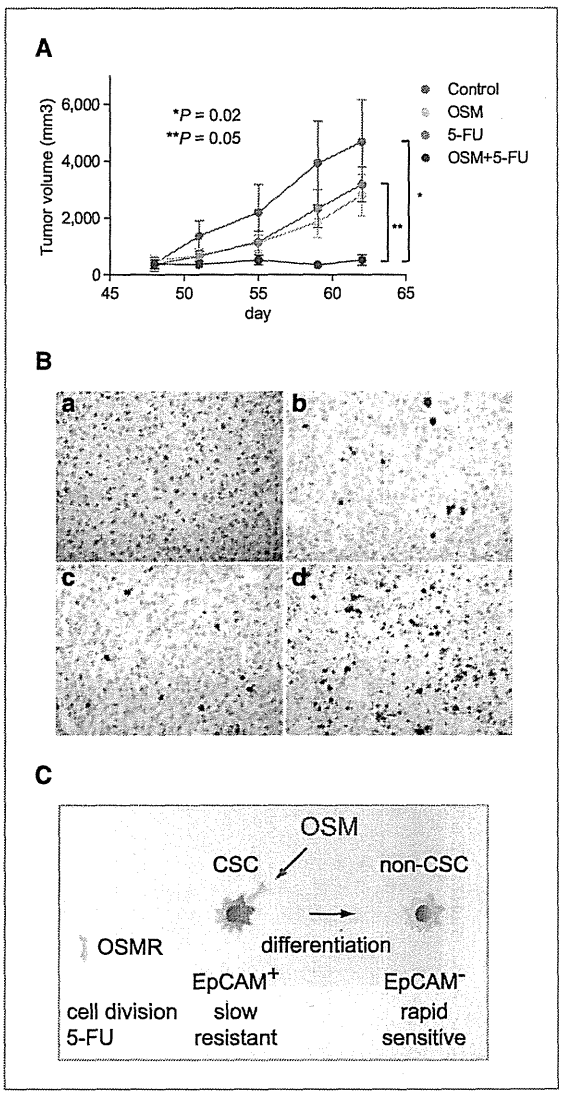

Figure 5. A, effect of PBS, OSM, 5-FU, and OSM plus 5-FU injections on the growth of primary EpCAM+ AFP+ HCC xenograft tumors in NOD/SCID mice (n = 4 in each group). Intratumoral injection of 50 μL of PBS, OSM (2 μg/tumor), 5-FU (250 μg/tumor), or OSM (2 μg/tumor) and 5-FU (250 μg/tumor) was initiated 48 days after transplantation, twice per week. B, representative images of activated caspase 3 staining of xenograft tumors in each treatment group (a, PBS; b, OSM; c, 5-FU; and d, OSM and 5-FU). C, a schematic diagram of the effect of OSM on EpCAM+ liver CSCs. Dormant EpCAM+ liver CSCs with OSMR expression respond to OSM and differentiate into rapidly dividing EpCAM- non-CSCs that are highly sensitive to 5-FU.

Published OnlineFirst May 18, 2010; DOI:10.1158/0008-5472.CAN-09-4210

high serum AFP, frequent EpCAM positivity, and poorly differentiated morphology, suggesting that OSMR is more likely expressed in HCC with stem/progenitor cell features (16). Although the regulatory mechanisms of OSMR are still unclear, it is plausible that OSMR expression is regulated by a signaling pathway activated during the process of hepatogenesis. Because gp130 is known to be ubiquitously expressed, regulation of OSM signaling might be largely dependent on the expression status of OSMR in normal and tumor tissues. Recent studies have shown the potential role of methylation of CpG islands located in OSMR promoter in colorectal cancer (31, 32). Clarification of OSMR promoter activity regulation, including CpG methylation, might provide clues for better understanding of hepatocytic differentiation signaling in both normal hepatic stem cells and CSCs.

It has been postulated that both normal stem cells and CSCs are dormant and show slow cell cycles. Consistent with this, CSCs are considered to be more resistant to chemotherapeutic agents than non-CSCs, possibly due to slow cell cycles as well as an increased expression of ATP-binding cassette transporters, robust DNA damage responses, and activated antiapoptotic signaling (20, 33, 34). Therefore, development of an effective strategy by targeting CSC pools together with conventional chemotherapies is essential to eradicate a tumor mass. Two strategies have been investigated to reduce the CSCs population in the tumor; that is, inhibition of self-renewal programs and activation of differentiation programs. We have shown that hepatocytic differentiation of liver CSCs by OSM results in enhanced cell proliferation *in vitro*. We have further shown here that OSM-mediated hepatocytic differentiation of liver CSCs in combination with conventional chemotherapy effectively suppresses HCC growth. It is possible that OSM may boost antitumor activity of 5-FU by "exhausting dormant CSCs" through hepatocytic differentiation and active cell division. It is encouraging that similar success with differentiation therapy has recently been reported in several cancers (24, 35, 36). In addition, HNF4-α–mediated differentiation of HCC cells has recently been reported to be effective for the eradication of HCC (37). However, although the combination of OSM and 5-FU effectively inhibited tumor growth in our model, we could not observe the shrinkage of the tumor. Thus, induction of CSC's differentiation with eradication of non-CSCs might not be enough for the eradication of the tumor, which might suggest the importance of inhibiting self-renewal as well as stimulating differentiation of CSCs. Because we induced the hepatocytic differentiation of the subcutaneous tumor by local injection of OSM, further rigorous studies are clearly required to assess the effect of OSM on liver CSCs and its utility for differentiation therapy in HCC.

CSCs may acquire resistance against differentiation therapy by additional genetic/epigenetic changes during treatment by clonal evolution, as observed in conventional chemotherapy. Indeed, it has recently been suggested that bone morphogenetic protein–mediated brain CSC differentiation failed in a subset of brain tumors in which bone morphogenetic protein receptor promoters were methylated and silenced (23). Similarly, OSMR silencing by promoter methylation might result in the development of OSM-resistant clones in HCC.

In conclusion, OSMR is expressed in certain types of HCC with stem/progenitor cell features, and OSM induces hepatocytic differentiation and active cell division of $OSMR^+$ liver CSCs to enhance chemosensitivity to 5-FU. The clinical safety and utility of OSM should be evaluated in the near future.

Disclosure of Potential Conflicts of Interest

No potential conflicts of interest were disclosed.

Acknowledgments

We thank Masayo Baba and Nami Nishiyama for excellent technical assistance.

Grant Support

Ministry of Education, Culture, Sports, Science and Technology, Japan grant-in-aid (no. 20599005).

The costs of publication of this article were defrayed in part by the payment of page charges. This article must therefore be hereby marked *advertisement* in accordance with 18 U.S.C. Section 1734 solely to indicate this fact.

Received 11/17/2009; revised 03/12/2010; accepted 03/31/2010; published OnlineFirst 05/18/2010.

References

1. Fialkow PJ. Clonal origin of human tumors. Biochim Biophys Acta 1976;458:283–321.
2. Clarke MF, Dick JE, Dirks PB, et al. Cancer stem cells—perspectives on current status and future directions: AACR Workshop on Cancer Stem Cells. Cancer Res 2006;66:9339–44.
3. Jordan CT, Guzman ML, Noble M. Cancer stem cells. N Engl J Med 2006;355:1253–61.
4. Al-Hajj M, Wicha MS, Benito-Hernandez A, Morrison SJ, Clarke MF. Prospective identification of tumorigenic breast cancer cells. Proc Natl Acad Sci U S A 2003;100:3983–8.
5. Bonnet D, Dick JE. Human acute myeloid leukemia is organized as a hierarchy that originates from a primitive hematopoietic cell. Nat Med 1997;3:730–7.
6. O'Brien CA, Pollett A, Gallinger S, Dick JE. A human colon cancer cell capable of initiating tumour growth in immunodeficient mice. Nature 2007;445:106–10.
7. Ricci-Vitiani L, Lombardi DG, Pilozzi E, et al. Identification and expansion of human colon-cancer-initiating cells. Nature 2007;445:111–5.
8. Singh SK, Hawkins C, Clarke ID, et al. Identification of human brain tumour initiating cells. Nature 2004;432:396–401.
9. Visvader JE, Lindeman GJ. Cancer stem cells in solid tumours: accumulating evidence and unresolved questions. Nat Rev Cancer 2008;8:755–68.
10. El-Serag HB, Rudolph KL. Hepatocellular carcinoma: epidemiology and molecular carcinogenesis. Gastroenterology 2007;132:2557–76.
11. Mishra L, Banker T, Murray J, et al. Liver stem cells and hepatocellular carcinoma. Hepatology 2009;49:318–29.
12. Chiba T, Kita K, Zheng YW, et al. Side population purified from hepatocellular carcinoma cells harbors cancer stem cell-like properties. Hepatology 2006;44:240–51.

Published OnlineFirst May 18, 2010; DOI:10.1158/0008-5472.CAN-09-4210

13. Ma S, Chan KW, Hu L, et al. Identification and characterization of tumorigenic liver cancer stem/progenitor cells. Gastroenterology 2007;132:2542–56.
14. Yang ZF, Ho DW, Ng MN, et al. Significance of CD90+ cancer stem cells in human liver cancer. Cancer Cell 2008;13:153–66.
15. Yang W, Yan HX, Chen L, et al. Wnt/β-catenin signaling contributes to activation of normal and tumorigenic liver progenitor cells. Cancer Res 2008;68:4287–95.
16. Yamashita T, Forgues M, Wang W, et al. EpCAM and α-fetoprotein expression defines novel prognostic subtypes of hepatocellular carcinoma. Cancer Res 2008;68:1451–61.
17. Yamashita T, Budhu A, Forgues M, Wang XW. Activation of hepatic stem cell marker EpCAM by Wnt-β-catenin signaling in hepatocellular carcinoma. Cancer Res 2007;67:10831–9.
18. Yamashita T, Ji J, Budhu A, et al. EpCAM-positive hepatocellular carcinoma cells are tumor-initiating cells with stem/progenitor cell features. Gastroenterology 2009;136:1012–24.
19. Boman BM, Huang E. Human colon cancer stem cells: a new paradigm in gastrointestinal oncology. J Clin Oncol 2008;26:2828–38.
20. Dean M, Fojo T, Bates S. Tumour stem cells and drug resistance. Nat Rev Cancer 2005;5:275–84.
21. Zou GM. Cancer initiating cells or cancer stem cells in the gastrointestinal tract and liver. J Cell Physiol 2008;217:598–604.
22. Hill RP, Perris R. "Destemming" cancer stem cells. J Natl Cancer Inst 2007;99:1435–40.
23. Lee J, Son MJ, Woolard K, et al. Epigenetic-mediated dysfunction of the bone morphogenetic protein pathway inhibits differentiation of glioblastoma-initiating cells. Cancer Cell 2008;13:69–80.
24. Piccirillo SG, Reynolds BA, Zanetti N, et al. Bone morphogenetic proteins inhibit the tumorigenic potential of human brain tumour-initiating cells. Nature 2006;444:761–5.
25. Nasr R, Guillemin MC, Ferhi O, et al. Eradication of acute promyelocytic leukemia-initiating cells through PML-RARA degradation. Nat Med 2008;14:1333–42.
26. Kamiya A, Kinoshita T, Ito Y, et al. Fetal liver development requires a paracrine action of oncostatin M through the gp130 signal transducer. EMBO J 1999;18:2127–36.
27. Kinoshita T, Miyajima A. Cytokine regulation of liver development. Biochim Biophys Acta 2002;1592:303–12.
28. Yamashita T, Honda M, Takatori H, et al. Activation of lipogenic pathway correlates with cell proliferation and poor prognosis in hepatocellular carcinoma. J Hepatol 2009;50:100–10.
29. Lobo NA, Shimono Y, Qian D, Clarke MF. The biology of cancer stem cells. Annu Rev Cell Dev Biol 2007;23:675–99.
30. Heinrich PC, Behrmann I, Haan S, Hermanns HM, Muller-Newen G, Schaper F. Principles of interleukin (IL)-6-type cytokine signalling and its regulation. Biochem J 2003;374:1–20.
31. Deng G, Kakar S, Okudiara K, Choi E, Sleisenger MH, Kim YS. Unique methylation pattern of oncostatin m receptor gene in cancers of colorectum and other digestive organs. Clin Cancer Res 2009; 15:1519–26.
32. Kim MS, Louwagie J, Carvalho B, et al. Promoter DNA methylation of oncostatin m receptor-β as a novel diagnostic and therapeutic marker in colon cancer. PLoS One 2009;4:e6555.
33. Bao S, Wu Q, McLendon RE, et al. Glioma stem cells promote radioresistance by preferential activation of the DNA damage response. Nature 2006;444:756–60.
34. Viale A, De Franco F, Orleth A, et al. Cell-cycle restriction limits DNA damage and maintains self-renewal of leukaemia stem cells. Nature 2009;457:51–6.
35. Gupta PB, Onder TT, Jiang G, et al. Identification of selective inhibitors of cancer stem cells by high-throughput screening. Cell 2009; 138:645–59.
36. Sipkins DA. Rendering the leukemia cell susceptible to attack. N Engl J Med 2009;361:1307–9.
37. Yin C, Lin Y, Zhang X, et al. Differentiation therapy of hepatocellular carcinoma in mice with recombinant adenovirus carrying hepatocyte nuclear factor-4α gene. Hepatology 2008;48:1528–39.

Liver INTERNATIONAL
OFFICIAL JOURNAL OF THE INTERNATIONAL ASSOCIATION FOR THE STUDY OF THE LIVER

Liver International ISSN 1478-3223

CLINICAL STUDIES

dUTP pyrophosphatase expression correlates with a poor prognosis in hepatocellular carcinoma

Hajime Takatori[1], Taro Yamashita[1], Masao Honda[1], Ryuhei Nishino[1], Kuniaki Arai[1], Tatsuya Yamashita[1], Hiroyuki Takamura[2], Tetsuo Ohta[2], Yoh Zen[3] and Shuichi Kaneko[1]

1 Department of Gastroenterology, Kanazawa University Graduate School of Medical Science, Ishikawa, Japan
2 Department of Gastroenterologic Surgery, Kanazawa University Graduate School of Medical Science, Ishikawa, Japan
3 Pathology Section, Kanazawa University Hospital, Ishikawa, Japan

Keywords
dUTP pyrophosphatase – hepatocellular carcinoma – prognosis – serial analysis of gene expression

Abbreviations
5-FU, 5-fluorouracil; dUTPase, dUTP pyrophosphatase; HCC, hepatocellular carcinoma; IHC, immunohistochemistry; qRT-PCR, quantitative reverse transcription-polymerase chain reaction; SAGE, serial analysis of gene expression.

Correspondence
Masao Honda, MD, Department of Gastroenterology, Kanazawa University Graduate School of Medical Science, 13-1 Takara-Machi, Kanazawa, Ishikawa 920-8641, Japan
Tel: +81 76 265 2233
Fax: +81 76 234 4250
e-mail: mhonda@m-kanazawa.jp

Received 13 August 2009
Accepted 26 October 2009

DOI:10.1111/j.1478-3231.2009.02177.x

Abstract

Background: Hepatocellular carcinoma (HCC) is a malignancy with a poor prognosis, partly owing to the lack of biomarkers that support its classification in line with its malignant nature. To discover a novel molecular marker that is related to the efficacy of treatment for HCC and its biological nature, we performed serial analysis of gene expression (SAGE) in HCC, normal liver and cirrhotic liver tissues. *Methods:* Gene expression profiles of HCC tissues and non-cancerous liver tissues were obtained by SAGE. Suppression of the target gene by RNA interference was used to evaluate its role in HCC *in vitro*. The relation of the identified marker and prognosis was statistically examined in surgically resected HCC patients. *Results:* We identified significant over-expression of *DUT*, which encodes dUTP pyrophosphatase (dUTPase), in HCC tissue, and this was confirmed in about two-thirds of the HCC samples by reverse-transcription polymerase chain reaction ($n=20$). Suppression of dUTPase expression using short interfering RNAs inhibited cell proliferation and sensitized HuH7 cells to 5-fluorouracil treatment. Nuclear dUTPase expression was observed in 36.6% of surgically resected HCC samples ($n=82$) evaluated by immunohistochemistry, and its expression was significantly correlated with the histological grades ($P=0.0099$). Notably, nuclear dUTPase expression correlated with a poor prognosis with statistical significance (HR, 2.47; 95% CI, 1.08–5.66; $P=0.032$). *Conclusion:* Taken together, these results suggest that nuclear dUTPase may be a good biomarker for predicting prognosis in HCC patients after surgical resection. Development of novel dUTPase inhibitors may facilitate the eradication of HCC.

Hepatocellular carcinoma (HCC) is the fifth most common malignancy and the third leading cause of cancer-related death worldwide (1). Several risk factors are responsible for HCC development, including alcoholism, aflatoxin and genetic diseases such as haemochromatosis and α-1 antitrypsin deficiency; however, the major risk factor is chronic hepatitis owing to hepatitis B virus (HBV) or hepatitis C virus (HCV) infection (2–4). Several treatment options are currently available for HCC management, which include liver transplantation, surgical resection, percutaneous ethanol injection, radio-frequency ablation, transcatheter arterial chemoembolization and systemic or local chemotherapy, and optimal treatment is determined based on tumour stage and liver function (5, 6). However, more than 80% of HCC cases develop advanced HCC after initial treatment (7).

Various chemotherapeutic drugs have been investigated for their antitumour activity in advanced HCC. For example, 5-fluorouracil (5-FU), a thymidylate synthase inhibitor, was the first reported drug studied for the treatment of advanced HCC; however, a median survival rate of 3–5 months has discouraged the further use of 5-FU as a single chemotherapeutic agent (8, 9). Interferon-α (IFN-α) has been reported to have antitumour activity against advanced HCC, and recent reports have suggested the efficacy of a combination of 5-FU/IFN-α for advanced HCC treatment (10–12), although convincing evidence for improved survival rate remains lacking. A recent study has indicated that 16% of advanced HCC patients responded positively to 5-FU/IFN-α treatment with clear and significant survival benefits compared with stable or progressive disease